

Asymptotically Accurate 3-D Recovery from Reissner-like Composite Plate Finite Elements

Wenbin Yu*, Dewey H. Hodges[†], and Vitali V. Volovoi[‡]
Georgia Institute of Technology, Atlanta, Georgia 30332-0150

An accurate stress/strain recovery procedure for laminated, composite plates that can be implemented in standard finite element programs is developed. The formulation is based on an asymptotic analysis and starts from a three-dimensional, anisotropic elasticity problem that takes all possible deformation into account. After a change of variable, which introduces intrinsic two-dimensional description for the deformation of the reference plane, the variational asymptotic method is then used to rigorously split this three-dimensional problem into two reduced-dimensional problems: a nonlinear, two-dimensional analysis of the reference surface of the deformed plate (an equivalent single-layer plate model), and a linear, one-dimensional analysis of the normal-line element through the thickness. The latter is solved by a one-dimensional finite element method and provides a constitutive law between the generalized, two-dimensional strains and stress resultants for the plate analysis, and a set of recovering relations to approximately express the three-dimensional displacement, strain and stress fields in terms of two-dimensional variables determined from solving the equations of the plate analysis. The strain energy functional that is asymptotically correct through the second order in the small parameters is then cast into the form of Reissner's theory. Although it is not in general possible to construct an asymptotically correct Reissner-like composite plate theory, an optimization procedure is used to drive the present theory as close as possible to being asymptotically correct, while maintaining the simplicity and beauty of the Reissner-like formulation. A computer program based on the present procedure, called Variational Asymptotic Plate and Shell Analysis (VAPAS), has been developed. Its utility is demonstrated by inserting the recovery procedure into the plate element of a general-purpose finite element code. Numerical results obtained for a variety of laminated, composite plates show that three-dimensional field variables recovered from the present theory agree very well with those from exact solutions.

*Graduate Research Assistant, School of Aerospace Engineering. Presently, Post Doctoral Fellow.

[†]Professor, School of Aerospace Engineering.

[‡]Research Engineer, School of Aerospace Engineering.

Introduction

Although composite materials have found increasing applications in aerospace engineering due to their superior engineering properties and enhanced manufacturing technology, their application is not so extensive as one could expect. One reason is that treatment of composite materials greatly complicates structural analysis. The old tools used for design of structures made of isotropic materials are no longer suitable for analyzing composite structures. Although many new models have appeared in the literature, design engineers have been reluctant to accept them with confidence. This is partly because many new models are constructed for specific problems without generalization in mind and partly because some models are too complicated and computationally inefficient to be used for design purposes. Simple yet efficient and generalized methods of analysis are still needed to shorten the design period and reduce the cost of composite structures.

Many engineering structures made with composite materials are flat panels having one dimension much smaller than the other two and can be modeled as plates. Plate models are generally derived from three-dimensional (3-D) elasticity theory, making use of an assumption that the plate is thin in some sense. The simplest composite plate theory is the classical lamination theory, which is based on the Kirchhoff hypothesis. It is well known, however, that composite plates do not have to be very thick in order for this theory to yield extremely poor results compared to the actual 3-D solution.

Although it is plausible to take into account the smallness of the thickness of such structures, construction of an accurate two-dimensional (2-D) model for a 3-D body still introduces a lot of challenges. There have been many attempts to rationally improve upon the classical model, almost all of which have serious shortcomings. One will appreciate this by reading several recent review papers [1–3]. Most of the models that have appeared in the literature [4–7] are based on *ad hoc* kinematic assumptions that cannot be reasonably justified for composite structures, such as an a priori distribution of displacement through the thickness.

From a mathematical point of view, the approximation in this dimensional reduction process stems from elimination of the thickness coordinate from the independent variables of the governing partial differential equations of equilibrium. This sort of approximation is inevitable if one wants to take advantage of the smallness of the thickness to simplify the analysis. However, other approximations that are not absolutely necessary should be avoided. For example, for small-strain analysis of plates and shells, it is reasonable to assume that the thickness, h , is small compared to the wavelength of deformation of the reference surface, l . However, it is not at all reasonable to assume a priori some *ad hoc* displacement field, although that is the way most plate theories are constructed.

In this paper we will proceed in a very different manner. We first cast the original 3-D

elasticity problem in a form that introduces intrinsic variables for the plate. This can be done in such a way as to be applicable for arbitrarily large displacement and global rotation, subject only to the strain being small [8,9]. Then, a systematic approach can be employed to reduce the dimensionality in terms of the smallness of h/l . The present work uses the Variational Asymptotic Method (VAM) [10] to split the original nonlinear 3-D elasticity problem into a linear, one-dimensional (1-D), normal-line analysis, and a nonlinear, 2-D, plate analysis. The normal-line analysis produces the 2-D constitutive law to be used in the 2-D plate analysis, along with recovering relations that yield the 3-D displacement, strain and stress fields using results obtained from the solution of the 2-D problem. The resulting 2-D plate theory is a geometrically-exact, equivalent single-layer theory in which the only generalized strains are three in-plane membrane strains, three out-of-plane curvature strains and two transverse shear strains. Such 2-D theories are termed herein as “Reissner-like.” However, this paper does not focus on the resulting 2-D theory, but instead on the through-the-thickness analysis. For this reason, there is no need to review here the extensive collection of published papers on 2-D plate theories. A detailed exposition of the 2-D theory implied by the dimensional reduction herein, and how it relates to existing 2-D theories can be found in [9].

The present work builds on previous work in [11–13]. This paper goes beyond [11] in three main ways:

1. The total energy is included in the present formulation while only the strain energy was dealt with in [11].
2. Transverse shear strain measures are introduced from the very beginning to obtain a Reissner-like model in [11]. On the other hand, in the present work the asymptotically correct refined energy is first obtained and then fit into a Reissner-like plate model.
3. A troublesome interaction term was dropped for convenience in [11], which causes the method introduced there to only give accurate results for homogeneous plates. Herein an optimization procedure is adopted here to derive the desired Reissner-like plate model as close to being asymptotically correct as possible.

The present approach differs the work of [12,13] at least in the following three aspects:

1. The theory introduced in [12,13] is restricted to be linear, while the present formulation is in an intrinsic form which is good for geometrically-exact nonlinear analysis.
2. A general form of the warping field is assumed *a priori* in [12,13], and the higher-order warping is used as a parameter to solve for unknown parameters in the assumed func-

tions. However, in the present work the warping field is solved by the usual procedures of the calculus of variations.

3. The theory of [12, 13] requires symbolic manipulation software such as Mathematica™ to obtain useful results, and it thus cannot be used in commercial finite element codes. On the other hand, the present approach is a completely different solution procedure, one which can be implemented in a 1-D finite element code (VAPAS) and can be easily inserted into the plate finite element formulations of standard finite element codes.

The authors note that the present paper is a companion paper to the purely analytical approach presented in [14]. Herein we use the finite element method to solve the normal-line analysis and connect the developed code, VAPAS, with DYMORE [15] to demonstrate its utility in standard finite element codes and provide an efficient and accurate analysis of composite plates.

3-D Formulation

A point in the plate can be described by its Cartesian coordinates x_i (see Fig. 1), where x_α are two orthogonal lines in the reference plane and x_3 is the normal coordinate. (Here and throughout the paper, Greek indices assume values 1 and 2 while Latin indices assume 1, 2, and 3. Repeated indices are summed over their range except where explicitly indicated.) Letting \mathbf{b}_i denote the unit vector along x_i for the undeformed plate, one can then describe the position of any material point in the undeformed configuration by its position vector $\hat{\mathbf{r}}$ from a fixed point O , such that

$$\hat{\mathbf{r}}(x_1, x_2, x_3) = \mathbf{r}(x_1, x_2) + x_3 \mathbf{b}_3 \quad (1)$$

where \mathbf{r} is the position vector from O to the point located by x_α on the reference plane. When the reference surface of the undeformed plate coincides with its middle surface, it naturally follows that

$$\langle \hat{\mathbf{r}}(x_1, x_2, x_3) \rangle = \mathbf{r}(x_1, x_2) \quad (2)$$

where the angle-brackets denote the definite integral through the thickness of the plate and will be used throughout the rest of the development.

When the plate deforms, the particle that had position vector $\hat{\mathbf{r}}$ in the undeformed state now has position vector $\hat{\mathbf{R}}$ in the deformed plate. The latter can be uniquely determined by the deformation of the 3-D body. Similarly, another triad \mathbf{B}_i is introduced for the deformed configuration. Note that the \mathbf{B}_i unit vectors are not necessarily tangent to the coordinates

of the deformed plate. The relation between \mathbf{B}_i and \mathbf{b}_i can be specified by an arbitrarily large rotation specified in terms of the matrix of direction cosines $C(x_1, x_2)$ so that

$$\mathbf{B}_i = C_{ij} \mathbf{b}_j \quad C_{ij} = \mathbf{B}_i \cdot \mathbf{b}_j \quad (3)$$

subject to the requirement that \mathbf{B}_i is coincident with \mathbf{b}_i when the structure is undeformed. Now the position vector $\hat{\mathbf{R}}$ can be represented as

$$\hat{\mathbf{R}}(x_1, x_2, x_3) = \mathbf{R}(x_1, x_2) + x_3 \mathbf{B}_3(x_1, x_2) + w_i(x_1, x_2, x_3) \mathbf{B}_i(x_1, x_2) \quad (4)$$

where w_i is the warping of the normal-line element. These quantities are not assumed, as in most plate theories. Rather, they are treated as unknown 3-D functions and will be solved for later. Eq. (4) is six times redundant because of the way warping introduced. Six constraints are needed to make the formulation unique. The redundancy can be removed by choosing appropriate definitions of \mathbf{R} and \mathbf{B}_i . Similar to the way \mathbf{r} is defined in Eq. (2), one can define \mathbf{R} to be the average position through the thickness. From this it follows that the warping functions must satisfy the three constraints

$$\langle w_i(x_1, x_2, x_3) \rangle = 0 \quad (5)$$

Another two constraints can be specified by taking \mathbf{B}_3 as the normal to the reference surface of the deformed plate. It should be noted that this choice has nothing to do with the famous Kirchhoff hypothesis. Indeed, it is only for convenience in the derivation. In the Kirchhoff assumption, no local deformation of the transverse normal is allowed. On the other hand, according to the present scheme we allow all possible deformation, classifying all deformation other than that of classical plate theory as warping, which is assumed to be small and to be solved by the VAM. This assumption is valid if the strain is small and the local rotation (*i.e.* the rotation of the normal line due to warping) is of the order of the strain or smaller [16].

Based on the concept of decomposition of rotation tensor [8,16], the Jauman-Biot-Cauchy strain components for small local rotation are given by

$$\Gamma_{ij} = \frac{1}{2}(F_{ij} + F_{ji}) - \delta_{ij} \quad (6)$$

where F_{ij} is the mixed-basis component of the deformation gradient tensor such that

$$F_{ij} = \mathbf{B}_i \cdot \mathbf{G}_k \mathbf{g}^k \cdot \mathbf{b}_j \quad (7)$$

Here $\mathbf{G}_k = \frac{\partial \hat{\mathbf{R}}}{\partial x_i}$ is the covariant basis vector of the deformed configuration and \mathbf{g}^k the contravariant base vector of the undeformed configuration and $\mathbf{g}^k = \mathbf{g}_k = \mathbf{b}_k$. One can obtain \mathbf{G}_k with the help of the definition of so-called generalized 2-D strains [11] given by

$$\mathbf{R}_{,\alpha} = \mathbf{B}_\alpha + \varepsilon_{\alpha\beta} \mathbf{B}_\beta \quad (8)$$

and

$$\mathbf{B}_{i,\alpha} = (-K_{\alpha\beta} \mathbf{B}_\beta \times \mathbf{B}_3 + K_{\alpha 3} \mathbf{B}_3) \times \mathbf{B}_i \quad (9)$$

where $\varepsilon_{\alpha\beta}$ and $K_{\alpha\beta}$ are the 2-D generalized strains and $(\cdot)_{,\alpha} = \frac{\partial(\cdot)}{\partial x_\alpha}$. There are no transverse shear strains appearing in Eq. (8) because we constrain \mathbf{B}_3 to be normal to the reference surface of the deformed plate. As mentioned previously, this serves the purpose of obtaining an asymptotically correct energy up to the second order. However, the transverse shear deformation is allowed, and its effects are included in the warping field. One is free to set $\varepsilon_{12} = \varepsilon_{21}$, *i.e.*

$$\mathbf{B}_1 \cdot \mathbf{R}_{,2} = \mathbf{B}_2 \cdot \mathbf{R}_{,1} \quad (10)$$

which can serve as another constraint to specify the deformed configuration.

With the assumption that the strain is small compared to unity, which has the effect of removing all the terms that are products of the warping and the generalized strains, one can express the 3-D strain field as

$$\Gamma = \Gamma_h w + \Gamma_\epsilon \epsilon + \Gamma_{l_1} w_{,1} + \Gamma_{l_2} w_{,2} \quad (11)$$

where

$$\Gamma = [\Gamma_{11} \quad 2\Gamma_{12} \quad \Gamma_{22} \quad 2\Gamma_{13} \quad 2\Gamma_{23} \quad \Gamma_{33}]^T \quad (12)$$

$$w = [w_1 \quad w_2 \quad w_3]^T \quad (13)$$

$$\epsilon = [\varepsilon_{11} \quad 2\varepsilon_{12} \quad \varepsilon_{22} \quad K_{11} \quad K_{12} + K_{21} \quad K_{22}]^T \quad (14)$$

and all the operators are defined as:

$$\begin{aligned}
\Gamma_h &= \begin{bmatrix} 0 & 0 & 0 \\ 0 & 0 & 0 \\ 0 & 0 & 0 \\ \frac{\partial}{\partial x_3} & 0 & 0 \\ 0 & \frac{\partial}{\partial x_3} & 0 \\ 0 & 0 & \frac{\partial}{\partial x_3} \end{bmatrix} & \Gamma_{l_1} &= \begin{bmatrix} 1 & 0 & 0 \\ 0 & 1 & 0 \\ 0 & 0 & 0 \\ 0 & 0 & 1 \\ 0 & 0 & 0 \\ 0 & 0 & 0 \end{bmatrix} \\
\Gamma_\epsilon &= \begin{bmatrix} 1 & 0 & 0 & x_3 & 0 & 0 \\ 0 & 1 & 0 & 0 & x_3 & 0 \\ 0 & 0 & 1 & 0 & 0 & x_3 \\ 0 & 0 & 0 & 0 & 0 & 0 \\ 0 & 0 & 0 & 0 & 0 & 0 \\ 0 & 0 & 0 & 0 & 0 & 0 \end{bmatrix} & \Gamma_{l_2} &= \begin{bmatrix} 0 & 0 & 0 \\ 1 & 0 & 0 \\ 0 & 1 & 0 \\ 0 & 0 & 0 \\ 0 & 0 & 1 \\ 0 & 0 & 0 \end{bmatrix}
\end{aligned} \tag{15}$$

Now, the strain energy of the plate per unit area (which is the same as the strain energy for the deformation of the normal-line element) can be written as

$$U = \frac{1}{2} \langle \Gamma^T D \Gamma \rangle \tag{16}$$

where D is the 3-D 6×6 material matrix, which consists of elements of the elasticity tensor expressed in the global coordinate system x_i . This matrix is in general fully populated. However, if it is desired to model laminated composite plates in which each lamina exhibits a monoclinic symmetry about its own mid-plane (for which the material matrix is determined by 13 constants instead of 21) and is rotated about the local normal to be a layer in the composite laminated plate, then as shown in [14], some parts of this material matrix will always vanish no matter what the layup angle is.

To deal with applied loads, we will at first leave open the existence of a potential energy and develop instead the virtual work of the applied loads. The virtual displacement is taken as the Lagrangean variation of the displacement field, such that

$$\delta \hat{\mathbf{R}} = \overline{\delta q_{B_i}} \mathbf{B}_i + x_3 \overline{\delta \psi_{B_i}} \mathbf{B}_i \times \mathbf{B}_3 + \delta w_i \mathbf{B}_i + \overline{\delta \psi_{B_i}} \mathbf{B}_i \times w_j \mathbf{B}_j \tag{17}$$

where the virtual displacement of the reference surface is given by

$$\overline{\delta q_{B_i}} = \delta \mathbf{u} \cdot \mathbf{B}_i \tag{18}$$

and the virtual rotation of the reference surface is defined such that

$$\delta \mathbf{B}_i = \overline{\delta \psi}_{B_j} \mathbf{B}_j \times \mathbf{B}_i \quad (19)$$

Since the strain is small, one may safely ignore products of the warping and the loading in the virtual rotation term. Then, the work done through a virtual displacement due to the applied loads $\tau_i \mathbf{B}_i$ at the top surface and $\beta_i \mathbf{B}_i$ at the bottom surface and body force $\phi_i \mathbf{B}_i$ through the thickness is

$$\overline{\delta W} = (\tau_i + \beta_i + \langle \phi_i \rangle) \overline{\delta q}_{B_i} + \overline{\delta \psi}_{B_\alpha} \left[\frac{h}{2} (\tau_\alpha - \beta_\alpha) + \langle x_3 \phi_\alpha \rangle \right] + \delta (\tau_i w_i^+ + \beta_i w_i^- + \langle \phi_i w_i \rangle) \quad (20)$$

where τ_i , β_i , and ϕ_i are taken to be independent of the deformation, $(\)^+ = (\)|_{x_3=\frac{h}{2}}$, and $(\)^- = (\)|_{x_3=-\frac{h}{2}}$. By introducing column matrices $\overline{\delta q}$, $\overline{\delta \psi}$, τ , β , and ϕ , which are formed by stacking the three elements associated with indexed symbols of the same names, and using Eqs. (1), (3), and (4), one may write the virtual work in matrix form, so that

$$\overline{\delta W} = \overline{\delta q}^T f + \overline{\delta \psi}^T m + \delta (\tau^T w^+ + \beta^T w^- + \langle \phi^T w \rangle) \quad (21)$$

where

$$f = \tau + \beta + \langle \phi \rangle$$

$$m = \left\{ \begin{array}{c} \frac{h}{2} (\tau_1 - \beta_1) + \langle x_3 \phi_1 \rangle \\ \frac{h}{2} (\tau_2 - \beta_2) + \langle x_3 \phi_2 \rangle \\ 0 \end{array} \right\} \quad (22)$$

The complete statement of the problem can now be presented in terms of the principle of virtual work, such that

$$\delta U - \overline{\delta W} = 0 \quad (23)$$

In spite of the possibility of accounting for nonconservative forces in the above, the problem that governs the warping is conservative. Thus, one can pose the problem that governs the warping as the minimization of a total potential functional

$$\Pi = U + W \quad (24)$$

so that

$$\delta \Pi = 0 \quad (25)$$

in which only the warping displacement is varied, subject to the constraints Eq. (5). This

implies that the potential of the applied loads for this portion of the problem is given by

$$W = -\tau^T w^+ - \beta^T w^- - \langle \phi^T w \rangle \quad (26)$$

Below, for simplicity of terminology, we will refer to Π as the total potential energy, or the total energy.

By principle of minimum total potential energy, one can solve the unknown warping functions by minimizing the functional in Eq. (24) subject to the constraints of Eq. (5). Up to this point, this is simply an alternative formulation of the original 3-D elasticity problem. If we attempt to solve this problem directly, we will meet the same difficulty as solving any full 3-D elasticity problem. Fortunately, as shown in [14], the VAM can be used to calculate the 3-D warping functions asymptotically. However, the minimization problem has been solved analytically in that work and the procedure becomes very tedious if there are lots of layers. Here a finite element discretization is used to solve the minimization problem. A 5-noded isoparametric element is used because we need the second-order warping functions, which are piecewise, fourth-order polynomials. Discretizing the transverse normal line into 1-D finite elements, one can express the warping field as

$$w(x_i) = S(x_3)V(x_1, x_2) \quad (27)$$

where S is the shape function and V is the nodal value of warping field along the transverse normal. Substituting Eq. (27) into Eq. (24), one can express the total energy in discretized form as

$$\begin{aligned} 2\Pi = & V^T E V + 2V^T (D_{he}\epsilon + D_{hl_1}V_{,1} + D_{hl_2}V_{,2}) \\ & + \epsilon^T D_{\epsilon\epsilon}\epsilon + V_{,1}^T D_{l_1 l_1} V_{,1} + V_{,2}^T D_{l_2 l_2} V_{,2} \\ & + 2(V_{,1}^T D_{l_1 \epsilon}\epsilon + V_{,2}^T D_{l_2 \epsilon}\epsilon + V_{,1}^T D_{l_1 l_2} V_{,2}) + 2V^T L \end{aligned} \quad (28)$$

where L contains the load related terms such that

$$L = -S^{+T}\tau - S^{-T}\beta - \langle S^T \phi \rangle \quad (29)$$

The new matrix variables carry the properties of both the geometry and material:

$$\begin{aligned}
E &= \langle [\Gamma_h S]^T D [\Gamma_h S] \rangle & D_{h\epsilon} &= \langle [\Gamma_h S]^T D \Gamma_\epsilon \rangle \\
D_{hl_1} &= \langle [\Gamma_h S]^T D [\Gamma_{l_1} S] \rangle & D_{hl_2} &= \langle [\Gamma_h S]^T D [\Gamma_{l_2} S] \rangle \\
D_{\epsilon\epsilon} &= \langle \Gamma_\epsilon^T D \Gamma_\epsilon \rangle & D_{l_1 l_1} &= \langle [\Gamma_{l_1} S]^T D [\Gamma_{l_1} S] \rangle \\
D_{l_1 l_2} &= \langle [\Gamma_{l_1} S]^T D [\Gamma_{l_2} S] \rangle & D_{l_2 l_2} &= \langle [\Gamma_{l_2} S]^T D [\Gamma_{l_2} S] \rangle \\
D_{l_1 \epsilon} &= \langle [\Gamma_{l_1} S]^T D \Gamma_\epsilon \rangle & D_{l_2 \epsilon} &= \langle [\Gamma_{l_2} S]^T D \Gamma_\epsilon \rangle
\end{aligned} \tag{30}$$

The discretized form of Eq. (5) is

$$V^T H \psi = 0 \tag{31}$$

where $H = \langle S^T S \rangle$ and ψ is the normalized kernel matrix of E such that $\psi^T H \psi = I$. Now our problem is transformed to minimize Eq. (28) numerically, subject to the constraints in Eq. (31).

Dimensional Reduction

Now, to rigorously reduce the original 3-D problem to a 2-D plate problem, one must attempt to reproduce the energy stored in the 3-D structure in a 2-D formulation. This dimensional reduction can only be done approximately, and one way to do it is by taking advantage of the smallness of h/l . Another small parameter is the order of the generalized 2-D strains ϵ which we denote here as ε and it has already been taken advantage of when we derive Eq. (11). One can observe that the first term of Eq. (11) has order $\frac{\|V\|}{h}$ and the last two terms have order $\frac{\|V\|}{l}$ which is clearly one order of h/l higher than the first term. This observation allows us to avoid dealing with derivatives of unknown functions with respect to in-plane coordinates. As mentioned before, although reduced-order models based on *ad hoc* kinematic assumptions regularly appear in the literature, there is no basis whatsoever to justify such assumptions. Rather, in this work, the VAM will be used to mathematically perform a dimensional reduction of the 3-D problem to a series of 2-D models. One can refer to [11] for a brief introduction of the VAM. To proceed by this method, one has to assess and keep track of the order of all the quantities in the formulation. Following [13], the quantities of interest have the following orders:

$$\epsilon_{\alpha\beta} \sim h \kappa_{\alpha\beta} \sim \varepsilon \quad f_3 \sim \mu (h/l)^2 \varepsilon \quad f_\alpha \sim \mu (h/l) \varepsilon \quad m_\alpha \sim \mu h (h/l) \varepsilon \tag{32}$$

where ε is the order of the maximum strain in the plate and μ is the order of the material constants (all of which are assumed to be of the same order). It is noted that $m_3 = 0$.

The VAM requires one to find the leading terms of the functional according to the different

orders. The total potential energy consists of quadratic expressions involving the warping and the generalized strains. In addition there are terms that involve the loading along with interaction terms between the warping and the both of the other types of quantities. Since only the warping is varied, one needs the leading term that involves warping only and the leading term that involves the warping and other quantities (*i.e.* the generalized strain and loading). For the zeroth-order approximation, these leading terms of Eq. (28) are

$$2\Pi_0^* = V^T E V + 2V^T D_{h\epsilon} \epsilon \quad (33)$$

The Euler-Lagrange equation for functional Eq. (33) subject to constraints Eq. (31) can be obtained by usual procedure of calculus of variation with the aid of a Lagrange multiplier as follows:

$$E V + D_{h\epsilon} \epsilon = H \psi \Lambda \quad (34)$$

Considering the properties of the kernel matrix ψ , one calculates the Lagrange multiplier Λ as

$$\Lambda = \psi^T D_{h\epsilon} \epsilon \quad (35)$$

Substituting Eq. (35) back into Eq. (34), we obtain

$$E V = (H \psi \psi^T - I) D_{h\epsilon} \epsilon \quad (36)$$

There exists a unique solution linearly independent of the null space of E for V because the right-hand-side of Eq. (36) is orthogonal to the null space. Since the solution is unique, we can choose any convenient constraints to make the problem determined. In our implementation, we arbitrarily constrain three degrees of freedom to obtain a solution V^* for the linear system, so that the final solution can be written as

$$V = V^* + \psi \lambda \quad (37)$$

where λ can be determined by Eq. (31) as

$$\lambda = -\psi^T H V^* \quad (38)$$

Hence the final solution minimizing the functional Eq. (28) subject to constraints Eq. (31) is

$$V = (I - \psi \psi^T H) V^* = \hat{V}_0 \epsilon = V_0 \quad (39)$$

Substituting Eq. (39) back into Eq. (28), one can obtain the total energy asymptotically

correct up to the order of $\mu\varepsilon^2$ as

$$2\Pi_0 = \epsilon^T (\hat{V}_0^T D_{h\epsilon} + D_{\epsilon\epsilon}) \epsilon \quad (40)$$

It is observed that the energy of this approximation coincides with classical laminated plate theories. However, we do not use *ad hoc* kinematic assumptions such as the Kirchhoff assumption to obtain this result. Although the energy is the same, the transverse normal strain from our zeroth-order approximation is not zero.

We notice that the zeroth-order warping is of order ε . According to the VAM, to accept this as the zeroth-order approximation, one needs to check whether or not the order of the next approximation is higher than this one. To obtain the first-order approximation, we simply perturb the zeroth-order result, resulting in warping functions of the form

$$V = V_0 + V_1 \quad (41)$$

Substituting Eq. (41) back into Eq. (11) and then into Eq. (28), one can obtain the leading terms for the first-order approximation as

$$2\Pi_1^* = V_1^T E V_1 + 2V_1^T D_1 \epsilon_{,1} + 2V_2^T D_2 \epsilon_{,2} + 2V_1^T L \quad (42)$$

where

$$D_1 = (D_{hl_1} - D_{hl_1}^T) \hat{V}_0 - D_{l_1\epsilon} \quad (43)$$

$$D_2 = (D_{hl_2} - D_{hl_2}^T) \hat{V}_0 - D_{l_2\epsilon} \quad (44)$$

It is understood that the order of the loads in Eq. (32) is associated with warping functions of different orders, as shown in [14]. For example, L in Eq. (42) only is composed of the in-plane components of the applied loads. Integration by parts with respect to the in-plane coordinates is used here and hereafter whenever it is convenient for the derivation, because the present goal is to obtain an interior solution for the plate without consideration of edge effects.

Similarly as in the zeroth-order approximation, one can solve the first-order warping field as

$$V_1 = V_{11}\epsilon_{,1} + V_{12}\epsilon_{,2} + V_{1L} \quad (45)$$

and obtain a total energy that is asymptotically correct up to the order of $\mu(h/l)^2\varepsilon$, given by

$$2\Pi_1 = \epsilon^T A \epsilon + \epsilon_{,1}^T B \epsilon_{,1} + 2\epsilon_{,1}^T C \epsilon_{,2} + \epsilon_{,2}^T D \epsilon_{,2} + 2\epsilon^T F + P \quad (46)$$

where

$$\begin{aligned}
A &= \hat{V}_0^T D_{h\epsilon} + D_{\epsilon\epsilon} & B &= \hat{V}_0^T D_{l_1 l_1} \hat{V}_0 + V_{11}^T D_1 \\
C &= \hat{V}_0^T D_{l_1 l_2} \hat{V}_0 + \frac{1}{2}(V_{11}^T D_2 + D_1^T V_{12}) & \mathcal{D} &= \hat{V}_0^T D_{l_2 l_2} \hat{V}_0 + V_{12}^T D_2 \\
F &= \hat{V}_0^T L - \frac{1}{2}(D_1^T V_{1L,1} + V_{11}^T L_{,1} + D_2^T V_{1L,2} + V_{12}^T L_{,2}) & P &= V_{1L}^T L
\end{aligned} \tag{47}$$

Here the monoclinic symmetry has already been taken advantage of to obtain the asymptotically correct energy in Eq. (46). It is noted that P is a quadratic term involving applied loads that cannot be varied in the 2-D model. When there is no load, this term vanishes. It comes from the applied load and the warping of refined approximations introduced by the applied load. The applied loads should not vary rapidly over the plate surface; otherwise, F will not be of sufficiently high order to meet the requirement of asymptotical correctness.

Transforming Into Reissner-like Model

Although Eq. (46) is asymptotically correct through the second order and straightforward use of this strain energy expression is possible as mentioned in [13], it involves more complicated boundary conditions than necessary since it contains derivatives of the generalized strain measures. To obtain an energy functional that is of practical use, one can transform the present approximation into a Reissner-like model.

In a Reissner-like model, there are two additional degrees of freedom, which are the transverse shear strains. These are incorporated into the rotation of transverse normal. If we introduce another triad \mathbf{B}_i^* for the deformed Reissner-like plate, the definition of 2-D strains becomes

$$\mathbf{R}_{,\alpha} = \mathbf{B}_\alpha^* + \varepsilon_{\alpha\beta}^* \mathbf{B}_\beta^* + 2\gamma_{\alpha 3} \mathbf{B}_3^* \tag{48}$$

$$\mathbf{B}_{i,\alpha}^* = (-K_{\alpha\beta}^* \mathbf{B}_\beta^* \times \mathbf{B}_3^* + K_{\alpha 3}^* \mathbf{B}_3^*) \times \mathbf{B}_i^* \tag{49}$$

where the transverse shear strains are $\gamma = [2\gamma_{13} \ 2\gamma_{23}]^T$. From the definitions in Eqs. (8) and (48), one can obtain the Rodrigues parameters corresponding to the rotation relating \mathbf{B}_i and \mathbf{B}_i^* . Using the procedures listed in [17], one can express the classical strain measures ϵ in terms of the strain measures of the Reissner-like plate model (see [18] for the details of the derivation):

$$\epsilon = \mathcal{R} - \mathcal{D}_\alpha \gamma_{,\alpha} \tag{50}$$

where

$$\begin{aligned}
\mathcal{D}_1 &= \begin{bmatrix} 0 & 0 & 0 & 1 & 0 & 0 \\ 0 & 0 & 0 & 0 & 1 & 0 \end{bmatrix}^T \\
\mathcal{D}_2 &= \begin{bmatrix} 0 & 0 & 0 & 0 & 1 & 0 \\ 0 & 0 & 0 & 0 & 0 & 1 \end{bmatrix}^T \\
\mathcal{R} &= [\varepsilon_{11}^* \quad 2\varepsilon_{12}^* \quad \varepsilon_{22}^* \quad K_{11}^* \quad K_{12}^* + K_{21}^* \quad K_{22}^*]^T
\end{aligned} \tag{51}$$

Now one can express the energy, Eq. (46), correct to second order, in terms of strains of the Reissner-like model as

$$2\Pi_1 = \mathcal{R}^T A \mathcal{R} - 2\mathcal{R}^T A \mathcal{D}_\alpha \gamma_{,\alpha} + \mathcal{R}_{,1}^T B \mathcal{R}_{,1} + 2\mathcal{R}_{,1}^T C \mathcal{R}_{,2} + \mathcal{R}_{,2}^T D \mathcal{R}_{,2} + 2\mathcal{R}^T F + P \tag{52}$$

The generalized Reissner-like model used in many 2-D analyses is of the form

$$2\Pi_{\mathcal{R}} = \mathcal{R}^T A \mathcal{R} + \gamma^T G \gamma + 2\mathcal{R}^T F_{\mathcal{R}} + 2\gamma^T F_{\gamma} \tag{53}$$

To find an equivalent Reissner model Eq. (53) for Eq. (52), one has to eliminate all partial derivatives of the classical 2-D strain measures. The equilibrium equations are used to achieve this purpose. From the two equilibrium equations balancing bending moments with applied moments m_α which is calculated from Eq. (22), one can obtain the following formula

$$G\gamma + F_\gamma = \mathcal{D}_1^T A \mathcal{R}_{,1} + \mathcal{D}_2^T A \mathcal{R}_{,2} + \begin{Bmatrix} m_1 \\ m_2 \end{Bmatrix} \tag{54}$$

Using Eq. (54), one can rewrite Eq. (52) as

$$2\Pi_1 = \mathcal{R}^T A \mathcal{R} + \gamma^T G \gamma + 2\mathcal{R}^T F + \bar{P} + U^* \tag{55}$$

where

$$U^* = \mathcal{R}_{,1}^T \bar{B} \mathcal{R}_{,1} + 2\mathcal{R}_{,1}^T \bar{C} \mathcal{R}_{,2} + \mathcal{R}_{,2}^T \bar{D} \mathcal{R}_{,2} \tag{56}$$

and

$$\begin{aligned}
\bar{B} &= B + A\mathcal{D}_1G^{-1}\mathcal{D}_1^T A \\
\bar{C} &= C + A\mathcal{D}_1G^{-1}\mathcal{D}_2^T A \\
\bar{D} &= D + A\mathcal{D}_2G^{-1}\mathcal{D}_2^T A \\
\bar{P} &= P - \begin{Bmatrix} m_1 \\ m_2 \end{Bmatrix}^T G^{-1} \begin{Bmatrix} m_1 \\ m_2 \end{Bmatrix}
\end{aligned} \tag{57}$$

If we can drive U^* to zero for any \mathcal{R} , then we have found an asymptotically correct Reissner-like plate model. For generally anisotropic plates, this term will not be zero; but we can minimize the error to obtain a Reissner-like model that is as close to asymptotical correctness as possible. The accuracy of the Reissner-like model depends on how close to zero one can drive this term of the energy.

One could proceed with the optimization at this point, but the problem will require a least squares solution for 3 unknowns (the shear stiffness matrix G) from a linear system of 78 equations (12×12 and symmetric). This optimization problem is too rigid. The solution will be better if we can bring more unknowns into the problem. As stated in [12], there is no unique plate theory of a given order. One can relax the constraints in Eq. (5) to be $\langle w_i \rangle = \text{const}$ and still obtain an asymptotically correct strain energy. Since the zeroth-order approximation gives us an asymptotic model corresponding to classical plate theory, we only relax the constraints for the first-order approximation. This relaxation will modify the warping field to be

$$\bar{V}_1 = V_{11}\epsilon_{,1} + V_{12}\epsilon_{,2} + V_{1L} + L_1\epsilon_{,1} + L_2\epsilon_{,2} \tag{58}$$

where L_1, L_2 consist of 24 constants. The remaining energy U^* will also be modified to be

$$U^* = \mathcal{R}_{,1}^T \hat{B} \mathcal{R}_{,1} + 2\mathcal{R}_{,1}^T \hat{C} \mathcal{R}_{,2} + \mathcal{R}_{,2}^T \hat{D} \mathcal{R}_{,2} \tag{59}$$

and

$$\hat{B} = \bar{B} + 2L_1^T D_1 \quad \hat{C} = \bar{C} + (L_1^T D_2 + D_1^T L_2) \quad \hat{D} = \bar{D} + 2L_2^T D_2 \tag{60}$$

Since now we have 27 unknowns, the optimization is much more flexible. It can give us a more optimal solution for the shear stiffness matrix G to fit the second-order, asymptotically-correct energy into a Reissner-like model. In other words, here we have found the Reissner-like model that describes as closely as possible the 2-D energy that is asymptotically correct through the second order in h/l . However, the asymptotical correctness of the warping field to

that same order can only be ascertained after obtaining another higher-order approximation, which will be discussed in the next section.

And after minimizing U^* , the total energy to be used for the 2-D plate solver can be expressed as:

$$2\Pi_{\mathcal{R}} = \mathcal{R}^T A \mathcal{R} + \gamma^T G \gamma + 2\mathcal{R}^T F \quad (61)$$

The quadratic term of loads \bar{P} is dropped from Eq. (55) because it will not affect the 2-D governing equations. It should be noted that the load-related terms in F are a new feature in the present development. One must slightly modify traditional Reissner-like plate solvers to accommodate these terms. This modification is not difficult and has a form similar to terms that must be included when considering thermal effects or actuated materials.

Recovering Relations

From the above, we have obtained a Reissner-like plate model which is as close as possible to being asymptotically correct in the sense of matching the total potential energy. The stiffness matrices A , G and load related term F can be used as input for a plate theory derived from the total energy obtained here. The geometrically nonlinear theory presented in [9] is an appropriate choice, but some straightforward modification of the loading terms is required.

However, while it is necessary to accurately calculate the 2-D displacement field of composite plates, this is not sufficient in many applications. Ultimately, *the fidelity of a reduced-order model such as this depends on how well it can predict the 3-D results in the original 3-D problem.* Hence, recovering relations should be provided to complete the reduced-order model. By recovering relations, we mean expressions for 3-D displacement, strain, and stress fields in terms of 2-D quantities and x_3 . For validation, results obtained for the 3-D field variables from the reduced-order model must be compared with those of the original 3-D model.

For a strain energy that is asymptotically correct through the second order, we can recover the 3-D displacement, strain and stress fields only through the first order in a strict sense of asymptotical correctness. Using Eqs. (1), (3), and (4), one can recover the 3-D displacement field through the first order as

$$U_{3d} = u_{2d} + x_3 \begin{bmatrix} C_{31} \\ C_{32} \\ C_{33} - 1 \end{bmatrix} + S V_0 + S \bar{V}_1 \quad (62)$$

where U_{3d} is the column matrix of 3-D displacements and u_{2d} is the plate displacements. C_{ij} are the components of global rotation tensor from Eq. (3). And from Eq. (11), one can

recover the 3-D strain field through the first order as

$$\Gamma = \Gamma_h S(V_0 + \bar{V}_1) + \Gamma_\epsilon \epsilon + \Gamma_{l_1} S V_{0,1} + \Gamma_{l_2} S V_{0,2} \quad (63)$$

Then, one can use the 3-D constitutive law to obtain 3-D stresses σ_{ij} .

Since we have obtained an optimum shear stiffness matrix G , some of the recovered 3-D results through the first order are better than classical theory and conventional first-order deformation theory. However, for the transverse normal component of strain and stress (*i.e.* Γ_{33} and σ_{33}), the agreement is not satisfactory at all. Let us recall, that the Reissner-like theory that has been constructed only ensures a good fit with the asymptotically correct 3-D displacement field of the first order (while energy is approximated to the second order). Thus, in order to obtain recovering relations that are valid to the same order as the energy, the VAM iteration needs to be applied one more time.

Using the same procedure listed in previous section, the second-order warping can be obtained and expressed symbolically as

$$V_2 = V_{21}\epsilon_{,11} + V_{22}\epsilon_{,12} + V_{23}\epsilon_{,22} \quad (64)$$

Eq. (64) is obtained by taking the original first-order warping V_1 to be the result of the first-order approximation. It is clear that V_2 is one order higher than V_1 which confirms that V_1 is the first-order approximation. One might be tempted to use V_1 in the recovering relations. However, the VAM has split the original 3-D problem into two sets of problems. As far as recovering relations concerned, it is observed that the normal-line analysis can at best give us an approximate shape of the distribution of 3-D results. The 2-D plate analysis will govern the global behavior of the structure. Since \bar{V}_1 is the warping that yields a Reissner-like plate model that is as close as possible to being asymptotically correct, we should still use \bar{V}_1 in the recovering relations instead of V_1 . By doing this, we choose to be more consistent with Reissner-like plate model while compromising somewhat on the asymptotical correctness of the shape of the distribution. It has been verified by numerical examples that this is a good choice.

Hence, we write the 3-D recovering relations for displacement through the second order as

$$U_{3d} = u_{2d} + x_3 \left\{ \begin{array}{c} C_{31} \\ C_{32} \\ C_{33} - 1 \end{array} \right\} + S(V_0 + \bar{V}_1 + V_2) \quad (65)$$

and the strain field through the second order is

$$\Gamma = \Gamma_h S(V_0 + \bar{V}_1 + V_2) + \Gamma_\epsilon \epsilon + \Gamma_{l_1} S(V_{0,1} + \bar{V}_{1,1}) + \Gamma_{l_2} S(V_{0,2} + \bar{V}_{1,2}) \quad (66)$$

Again the stresses through the second order can be obtained from use of the 3-D material law. It will be shown in the next section that the recovered 3-D results through the second order agree with the exact results very well.

Numerical Examples

A computer program, Variational Asymptotic Plate and Shell Analysis (VAPAS) based on the present theory has been developed. Several numerical examples are given here to validate the proposed theory and code developed based on this. First we investigate several cases for cylindrical bending problem of which the exact solutions have already been worked out by Pagano [19]. Then we study the vibration of laminated plates using a 2-D solver (here DYMORE is used) along with VAPAS to recover the 3-D fields at a specific time to compare the results with First-Order Shear Deformation Theory (FOSDT) [20].

Cylindrical bending problem for plate

In this section we give a few sample results to illustrate the power of the derived theory. The material properties of all plates studies in the section are

$$\begin{aligned} E_L &= 25 \times 10^6 \text{ psi} & E_T &= 10^6 \text{ psi} \\ G_{LT} &= 0.5 \times 10^6 \text{ psi} & G_{TT} &= 0.2 \times 10^6 \text{ psi} \\ \nu_{LT} &= \nu_{TT} = 0.25 \end{aligned}$$

where L denotes the direction parallel to the fibers and T the transverse direction. The test problem is a plate with width $L = 4$ in. along x_1 (the ‘‘lateral’’ direction) as sketched in Fig. 2 and infinite length in the x_2 direction (the ‘‘longitudinal’’ direction). The thickness of the plate is 1 in., so that the aspect ratio $L/h = 4$. The plate is simply supported and subjected to a sinusoidal surface loading of the form

$$\tau_3 = \beta_3 = \frac{p_0}{2} \sin\left(\frac{\pi x_1}{L}\right) \quad (67)$$

with $\tau_\alpha = \beta_\alpha = 0$. Three different cases of layups (the stacking sequence is from bottom to top) are investigated:

- case 1: antisymmetric angle ply, $[15^\circ / -15^\circ]$
- case 2: symmetric angle ply, $[30^\circ / -30^\circ / -30^\circ / 30^\circ]$

- case 3: symmetric nearly cross ply, $[0.5^\circ/90.5^\circ/90.5^\circ/0.5^\circ]$. The reason we change the ply angle a little bit from the cross-ply case is to allow us to use a Mathematica™ code we developed based on [19] which does not apply to cross-ply case.

Although our Reissner-like model is consistent with a geometrically-exact, nonlinear, 2-D plate theory such as in [9], only geometrically linear examples are considered herein for the purpose of comparing the results with the exact linear elasticity solutions of [19].

For the purpose of presenting the results graphically, the following normalization scheme is used:

$$\bar{\sigma}_{ij} = \frac{\sigma_{ij}}{p_0} \quad (68)$$

All six components of the 3-D stress along the thickness direction are presented. However, since the 3-D displacement field is usually of relatively little interest in analysis of composite plates, those results are not presented here. Similarly, the strain results are not presented for the sake of brevity since their accuracy is the same as that of the stresses. Note that, because the 2-D variables are either sine or cosine functions of x_1 , $\sigma_{\alpha\beta}$ and σ_{33} are plotted for the position $x_1 = L/2$, and $\sigma_{\alpha 3}$ are plotted for the position $x_1 = 0$ or $x_1 = L$.

First, we investigate a laminated composite plate with lay-up $[15^\circ / -15^\circ]$. The results of present theory (dashed line) plotted in Figs. 3 – 8 are compared with the exact solutions from [19] (solid line), classical theory (the zeroth-order approximation derived herein, dash-dotted line) and a similar yet very different theory in [12] (dotted line) which is referred to as the Sutyryn theory here. From the plotted results, one can observe that both the present theory and the Sutyryn theory have excellent agreement with the 3-D exact solution and produce much better results than the classical theory, especially for the transverse shear and transverse normal stresses.

Although there are significant differences between the present approach and that of [12], the results from both approaches are very close and have excellent agreement with 3-D exact solutions. However, [12] uses a so-called smart minimization procedure without a known mathematical basis to produce the good agreement obtained. If one simply applies the least squares technique as is done for the present theory, the accuracy of the results produced by the theory of [12] will be slightly degraded.

Next, we take another laminated composite plate with lay-up $[30^\circ / -30^\circ / -30^\circ / 30^\circ]$ and the same material properties as the previous plate. The results are shown in Figs. 9 – 14. The power of the present theory is clearly exhibited in the excellent agreement with exact 3-D solutions. Indeed, even though there are more layers in this example, the agreement is still excellent. Recall that the recovery relations use results from a standard Reissner-like plate model. The large number of degrees of freedom in layer-wise models depends on the

number of layers and is obviously not needed to achieve the level of accuracy shown here.

In case 3, we apply our technique to a very challenging lay-up $[0.5^\circ/90.5^\circ/90.5^\circ/0.5^\circ]$. The properties and behavior of a plate with this kind of lay-up are very close to those of a sandwich plate with a soft core. That the present theory can approximate the results very closely shows the present theory to be suitable for the modeling of such structures. The stress results are shown in Figs. 15 – 20. As one can observe from the results, even for this case, the present theory agrees very well with the exact solution. These results illustrate that one can use the present theory to model laminated plates confidently and get great accuracy with much less computational effort than layer-wise theories [21].

To demonstrate that the proposed theory and the code developed based the theory, namely VAPAS, can handle practical layups, we investigate the cylindrical bending problem for a composite plate with 20 layers with symmetric layup as $[30^\circ / - 30^\circ / - 30^\circ / 30^\circ]_5$ numbered from the bottom to the top. The Sutyryn theory cannot obtain the result for this case due to the prohibitive computational time. The FOSDT is used instead for comparison. The results are reported in Figs. 21 – 26. From the figures, one can observe that all the models (CLT: dash-dotted line; FOSDT: dashed line; VAPAS: dots) can produce reasonable predictions for the in-plane stress distribution through the thickness compared to the exact solution (solid line). VAPAS results are almost on the top of the exact solutions. Most significant, however, is the fact that VAPAS obtains much more accurate results for the transverse stress components. It should be noted that the computation can be done by VAPAS within one second in a personal computer.

It is to be expected that the present theory is far better than *ad hoc* models. Mathematically, the accuracy of the present theory should be comparable to that of a layer-wise plate theory with assumed in-plane displacements as layer-wise cubic polynomials of the thickness direction and transverse displacement as a layer-wise fourth-order polynomial. However, the present theory is still an equivalent single-layer theory, and the computational requirement is much less than layer-wise theories. Moreover, it is not necessary to use integration through the thickness of the 3-D equilibrium equations to get the transverse normal and transverse shear strain and stress results presented herein.

Vibration of Composite Plate Analyzed by DYMORE and VAPAS

VAPAS has been inserted into DYMORE to provide an efficient and accurate analysis for composite plates. VAPAS provides a generalized 2-D constitutive law for the input of DYMORE to carry out a 2-D analysis. Then VAPAS takes the output from DYMORE to recover the 3-D displacement, strain and stress fields.

To illustrate results from this procedure, vibration of a thick square composite plate of

width $w = 0.04$ m and thickness $h = 0.01$ m (see Fig. 27) is analyzed with DYMORE and VAPAS. The plate is clamped along edges BC and CD and free along the other two. A concentrated mass $M = 50$ kg is attached at point A . The plate is made of laminated composite material with a two-ply lay-up $[90, 0^\circ]$, where the 0° direction is parallel to the x_1 axis. Material properties for the composite are

$$\begin{aligned}
 E_1 &= 172.4 \text{ GPa} & E_2 &= E_3 = 6.9 \text{ GPa} \\
 G_{23} &= 1.38 \text{ GPa} & G_{12} &= G_{13} = 3.45 \text{ GPa} \\
 \rho &= 1600 \text{ kg/m}^3 & \nu_{12} &= \nu_{13} = \nu_{23} = 0.25
 \end{aligned} \tag{69}$$

The plate is subjected to a concentrated transverse load at point A . This load is a triangular impulse linearly rising to 10 kN in 0.001 s, then linearly decreasing to reach a zero value at time $t = 0.002$ s. The plate was modeled by a regular 12×12 mesh of quadratic elements and simulations were run with a constant time step $\Delta t = 10^{-4}$ sec.

Fig. 28 shows the time history of the displacements at mid-plane at point M ($x_1 = w/2, x_2 = w/2$). At time $t > 0.002$ s, the applied load vanishes so the plate shows free vibration behavior with period $T = 0.0332$ s. The time histories of the stresses through the thickness at M are shown in fig. 29. The recovered stress components show periodic behavior as expected. First and second derivatives of strain and curvature components are required for the recovering process of VAPAS. The higher-order strain derivatives were obtained by interpolating the strain values at the Gauss points of each of the four elements forming a 2×2 patch of elements around the recovering point.

At time $t = 0.0096$ s, the 3-D stress fields through the thickness of the plate were recovered at points M and Q ($x_1 = h, x_2 = w - h$) and using VAPAS and First-order Shear Deformation Theory (FOSDT) [20]. Note, however, that our FOSDT results are based on the shear stiffness matrix G obtained from VAPAS since the traditional FOSDT has no inherent means to obtain the shear stiffness coefficients for composite plates. These results are shown in Figs. 30 and 31 for the points M and Q , respectively. As expected, the theories predict values of in-plane stress components that are in good agreement with each other. However, the predictions for the interlaminar stresses components vary widely. Indeed, the FOSDT assumes constant transverse shear strain distributions and vanishing normal strains, whereas these strain components can be accurately predicted by VAPAS. Note that the predictions from VAPAS also satisfy the conditions of zero transverse shear and normal stresses at the top and bottom of the laminated plate.

Conclusion

A complete Reissner-like plate theory that is as close as possible to an asymptotically correct theory is developed for laminated, composite plates. The theory is applicable to plates for which each layer is made of monoclinic material. Although the resulting plate theory is as simple as a single-layer, FOSDT, the recovered 3-D displacement, strain and stress results have excellent accuracy, comparable to that of higher-order, layer-wise plate theories with many more degrees of freedom. The present paper has built on the work of several previous works mainly represented in [11–13]. The main contributions are as follows:

1. The present theory formulates the original 3-D elasticity problem in an intrinsic form which is suitable for geometrically nonlinear plate theory as well as linear theory.
2. The present theory solves the unknown 3-D warping functions asymptotically by using the variational asymptotic method and the principle of minimum total potential energy, a procedure which is systematic and easy to apply iteratively. In [12], the warping functions are calculated by an equivalent but involved analytical formulation.
3. The present theory finds a total potential energy instead of only the strain energy as presented in [11]. Having a total potential energy asymptotically correct to a certain order, one can derive a geometrically nonlinear plate theory in a straightforward manner using an energy method as done in [9].

A computer program, VAPAS, based on present theory has been developed and can calculate the generalized 2-D stiffness matrices (A , G , F) for analysis of nonlinear plate problems. This program can also recover the 3-D displacement/strain/stress fields with an accuracy comparable to that of layer-wise theory. Since VAPAS merely solves a 1-D problem, such a code executes very rapidly, enabling these very accurate recovering relations to be cheaply included in standard plate finite element codes. Also, since the kinematical foundation of the present theory is intrinsic, it is natural to extend the present theory to model composite shells, including inflatables. Such extensions of the present theory are under development and will be presented in future papers.

Acknowledgements

This research is supported by the Air Force Office of Scientific Research, USAF, under grant F49620-01-1-0038 (Maj. William M. Hilbun, technical monitor). The views and conclusions contained herein are those of the authors and should not be interpreted as necessarily representing the official policies or endorsement, either expressed or implied, of AFOSR or the U.S. Government. Technical discussions with Dr. Vladislav Sutyrin and our use of his

Mathematica™ codes for both the exact solution and his theory are greatly appreciated. Thanks are also due to Prof. Olivier A. Bauchau and Dr. Jou-Young Choi at Georgia Tech for permission to use results from their numerical example.

References

1. A. K. Noor and W. S. Burton, Assessment of shear deformation theories for multilayered composite plates. *Applied Mechanics Review*, 1989, **41**, 1 – 13.
2. A. K. Noor and W. S. Burton, Assessment of computational models for multilayered composite shells. *Applied Mechanics Review*, 1990, **43**.
3. A. K. Noor and M. Malik, An assessment of five modeling approaches for thermo-mechanical stress analysis of laminated composite panels. *Computational Mechanics*, 2000, **25**, 43–58.
4. J. N. Reddy, A simple higher-order theory for laminated composite plates. *Journal of Applied Mechanics*, 1984, **51**, 745 – 752.
5. M. Touratier, An efficient standard plate theory. *International Journal of Engineering Science*, 1991, **29**, 901 – 916.
6. M. DiSciuva, Development of anisotropic multilayered shear deformable rectangular plate element. *Computers and Structures*, 1985, **21**, 789 – 796.
7. Y. B. Cho and R. C. Averill, First-order zig-zag sublaminated plate theory and finite element model for laminated composite and sandwich panels. *Composite Structures*, 2000, **50**, 1 – 15.
8. D. A. DANIELSON, 1991, *Proceedings of the 2nd Pan American Congress of Applied Mechanics*, Valparaiso, Chile. Valparaiso Chile. Finite rotation with small strain in beams and plates.
9. D. H. Hodges, A. R. Atilgan and D. A. Danielson, A geometrically nonlinear theory of elastic plates. *Journal of Applied Mechanics*, 1993, **60**, 109 – 116.
10. V. L. Berdichevsky, Variational-asymptotic method of constructing a theory of shells. *PMM*, 1979, **43**, 664 – 687.
11. A. R. Atilgan and D. H. Hodges, On the strain energy of laminated composite plates. *International Journal of Solids and Structures*, 1992, **29**, 2527 – 2543.

12. V. G. Sutyryn and D. H. Hodges, On asymptotically correct linear laminated plate theory. *International Journal of Solids and Structures*, 1996, **33**, 3649 – 3671.
13. V. G. Sutyryn, Derivation of plate theory accounting asymptotically correct shear deformation. *Journal of Applied Mechanics*, 1997, **64**, 905 – 915.
14. W. Yu, D. H. Hodges and V. V. Volovoi, Asymptotic construction of Reissner-like models for composite plates with accurate strain recovery. To appear. *International Journal of Solids and Structures*, 2002, .
15. O. Bauchau, Computational schemes for flexible, nonlinear multi-body systems. *Multi-body System Dynamics*, 1998, **2**, 169–225.
16. D. A. Danielson and D. H. Hodges, Nonlinear beam kinematics by decomposition of the rotation tensor. *Journal of Applied Mechanics*, 1987, **54**, 258 – 262.
17. D. H. Hodges, Finite rotation and nonlinear beam kinematics. *Vertica*, 1987, **11**, 297 – 307.
18. W. YU, 2002, *Ph.D. dissertation, Aerospace Engineering, Georgia Institute of Technology*. Variational asymptotic modeling of composite dimensionally reducible structures.
19. N. J. Pagano, Influence of shear coupling in cylindrical bending of anisotropic laminates. *Journal of Composite Materials*, 1970, **4**, 330 – 343.
20. J. N. REDDY, *Mechanics of Laminated Composite Plates: Theory and Analysis*, CRC Press, Boca Raton, Florida, 1997.
21. D. H. Robbins and J. N. Reddy, Modeling of thick composites using a layerwise laminate theory. *International Journal for Numerical Methods in Engineering*, 1993, **36**, 655 – 677.

List of Figure Captions

- Figure 1: Schematic of plate deformation
- Figure 2: Cylindrical bending of composite plate
- Figure 3: σ_{11} vs the thickness coordinate (case 1)
- Figure 4: σ_{12} vs the thickness coordinate (case 1)
- Figure 5: σ_{22} vs the thickness coordinate (case 1)
- Figure 6: σ_{13} vs the thickness coordinate (case 1)
- Figure 7: σ_{23} vs the thickness coordinate (case 1)
- Figure 8: σ_{33} vs the thickness coordinate (case 1)
- Figure 9: σ_{11} vs the thickness coordinate (case 2)
- Figure 10: σ_{12} vs the thickness coordinate (case 2)
- Figure 11: σ_{22} vs the thickness coordinate (case 2)
- Figure 12: σ_{13} vs the thickness coordinate (case 2)
- Figure 13: σ_{23} vs the thickness coordinate (case 2)
- Figure 14: σ_{33} vs the thickness coordinate (case 2)
- Figure 15: σ_{11} vs the thickness coordinate (case 3)
- Figure 16: σ_{12} vs the thickness coordinate (case 3)
- Figure 17: σ_{22} vs the thickness coordinate (case 3)
- Figure 18: σ_{13} vs the thickness coordinate (case 3)
- Figure 19: σ_{23} vs the thickness coordinate (case 3)
- Figure 20: σ_{33} vs the thickness coordinate (case 3)
- Figure 21: σ_{11} vs the thickness coordinate (20 layers)
- Figure 22: σ_{12} vs the thickness coordinate (20 layers)
- Figure 23: σ_{22} vs the thickness coordinate (20 layers)
- Figure 24: σ_{13} vs the thickness coordinate (20 layers)
- Figure 25: σ_{23} vs the thickness coordinate (20 layers)

Figure 26: σ_{33} vs the thickness coordinate (20 layers)

Figure 27: Configuration of the clamped composite plate problem

Figure 28: Time history of displacements at mid-plane at point M . Vertical displacement U_3 – solid line; Lateral displacement U_1 – dashed line; Lateral displacement U_2 – dotted line

Figure 29: Time histories of the 3-D stress distribution along the thickness at the point M

Figure 30: Comparison of the 3-D stress distribution at point M . Dashed line – VAPAS; solid line – FOSDT

Figure 31: Comparison of the 3-D stress distribution at point Q . Dashed line – VAPAS; solid line – FOSDT

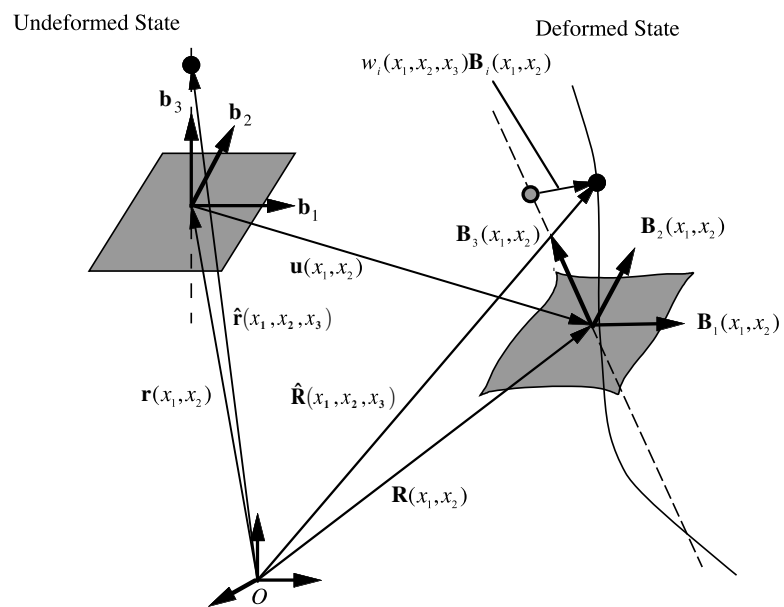


FIGURE 1:

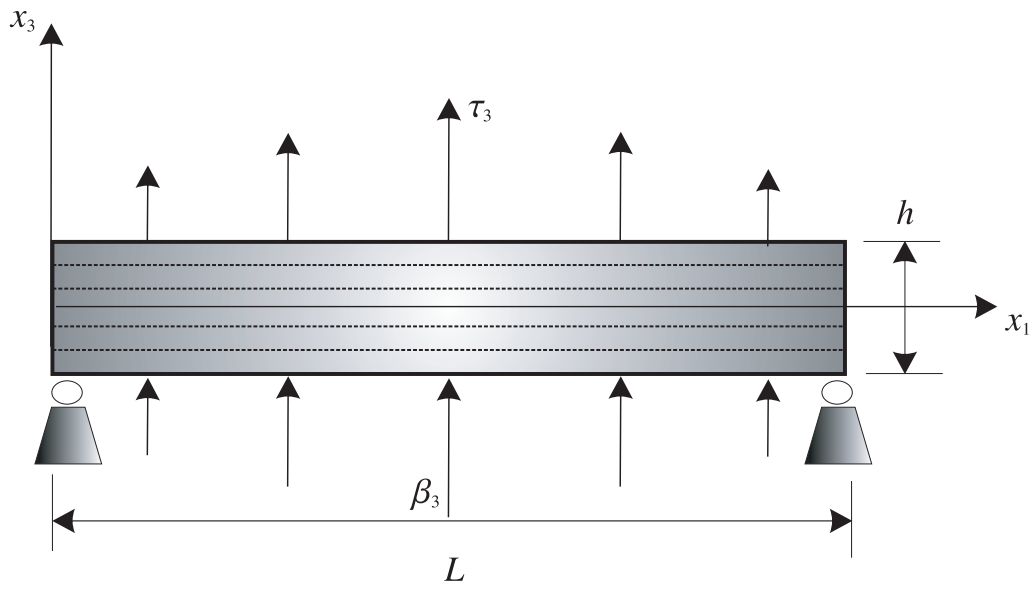


FIGURE 2:

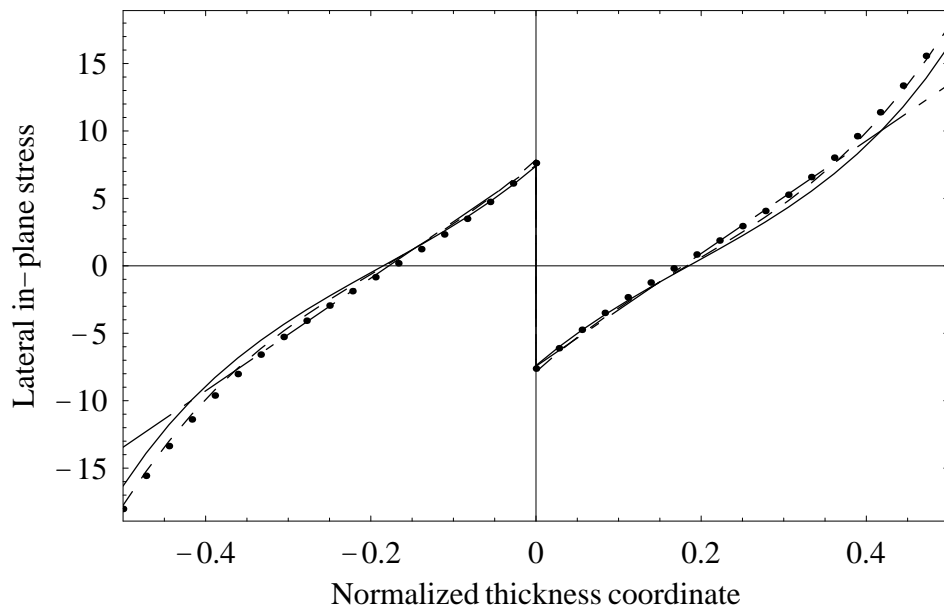


FIGURE 3:

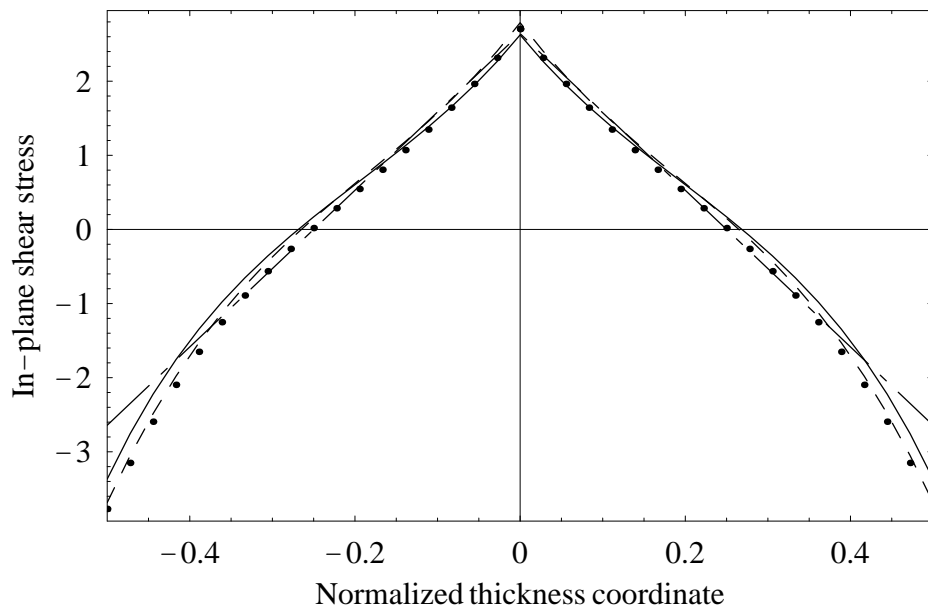


FIGURE 4:

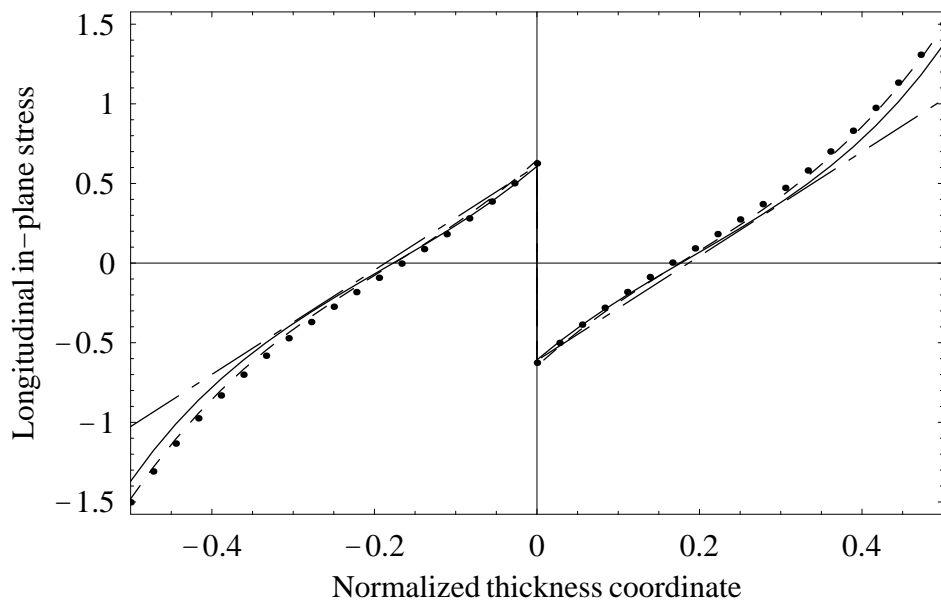


FIGURE 5:

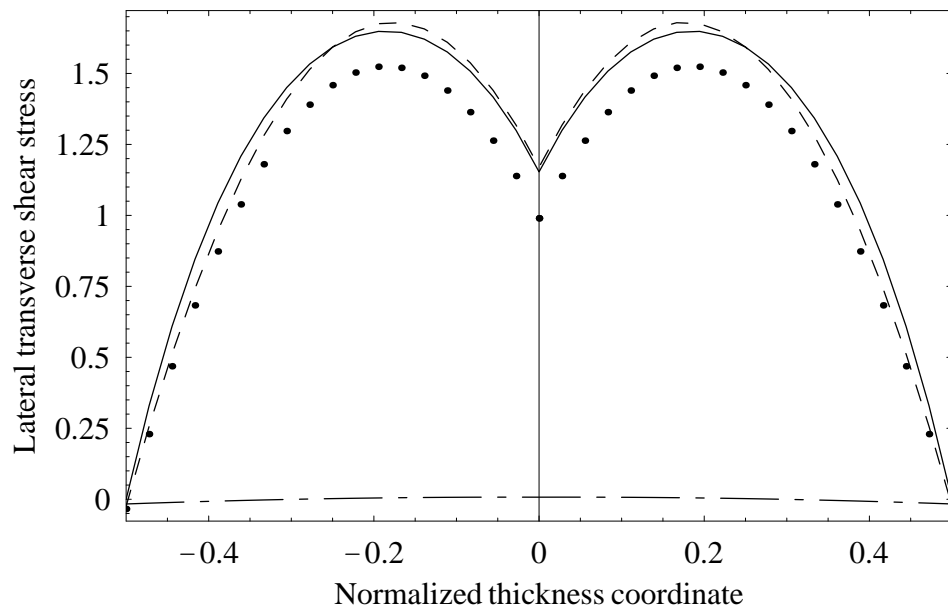


FIGURE 6:

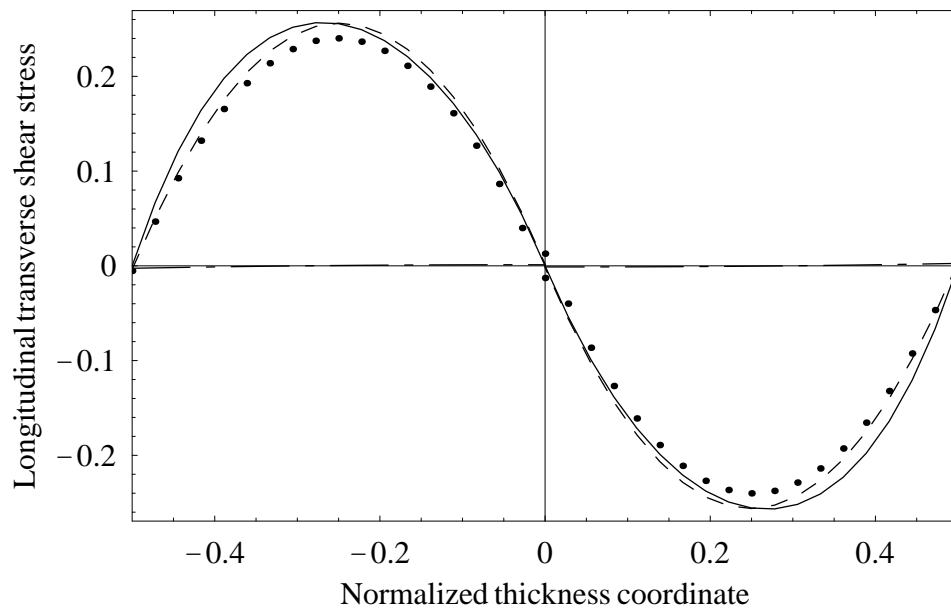


FIGURE 7:

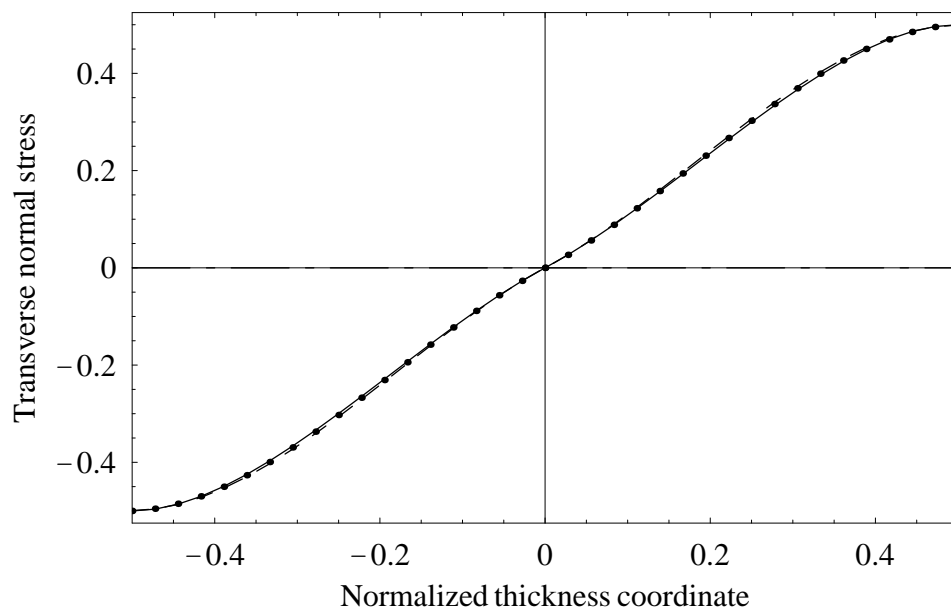


FIGURE 8:

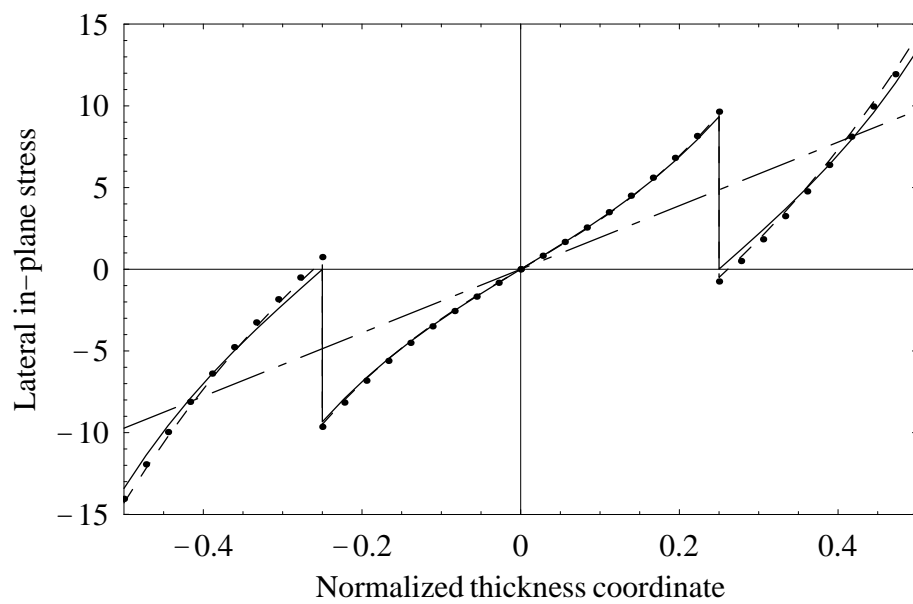


FIGURE 9:

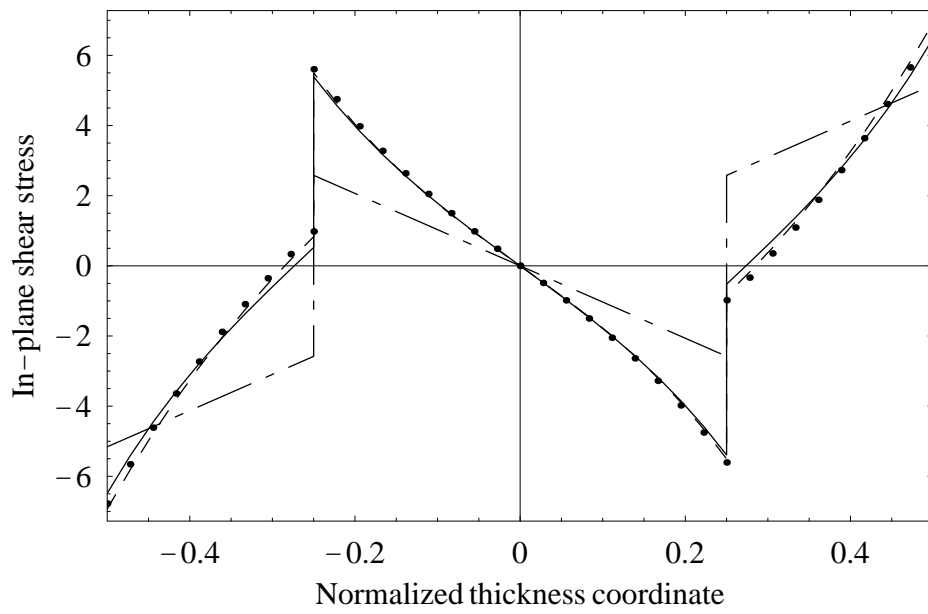


FIGURE 10:

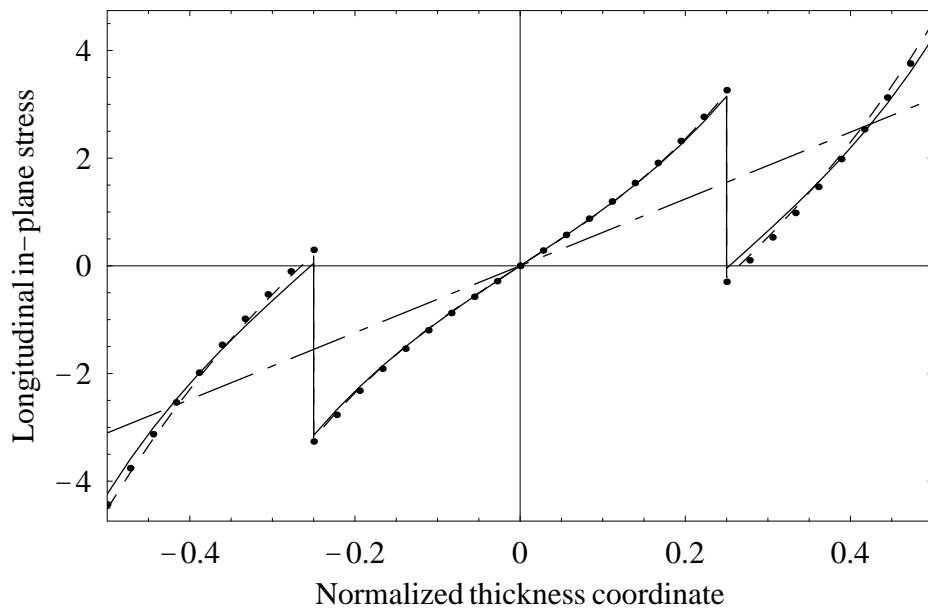


FIGURE 11:

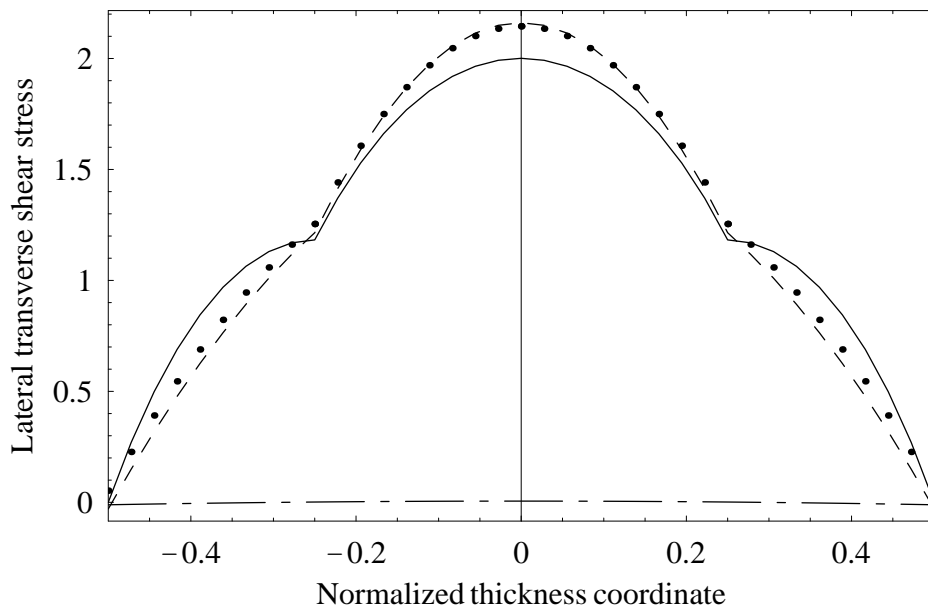


FIGURE 12:

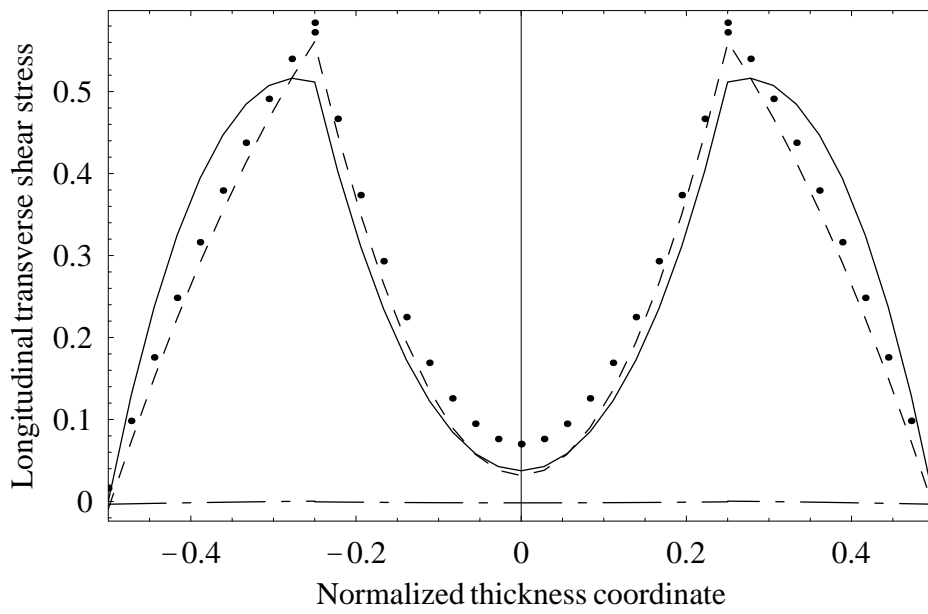


FIGURE 13:

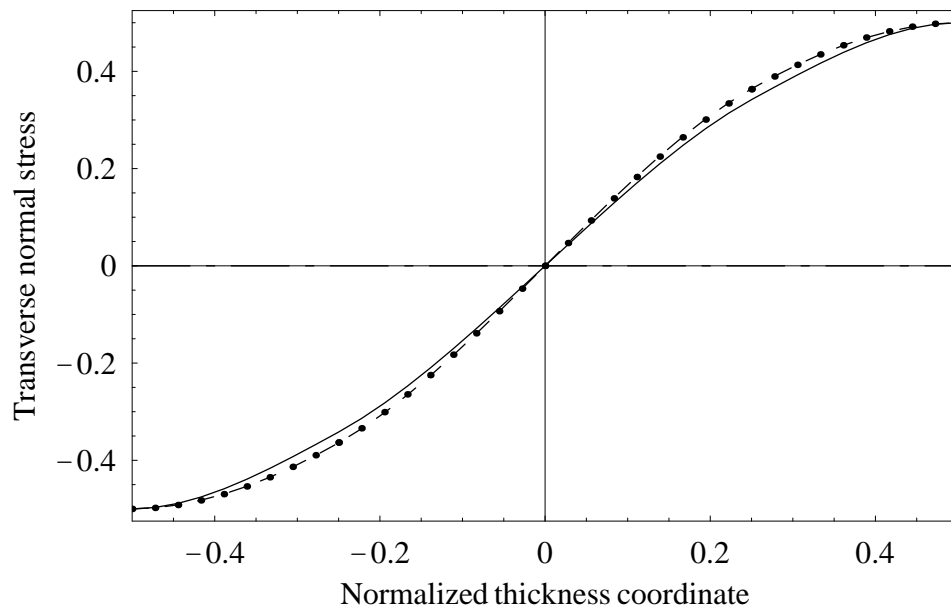


FIGURE 14:

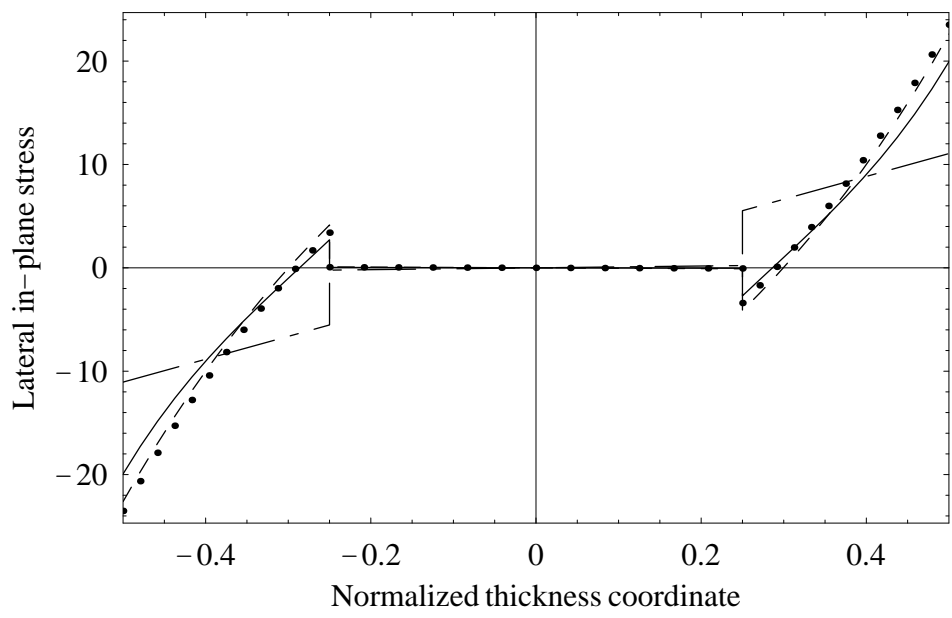


FIGURE 15:

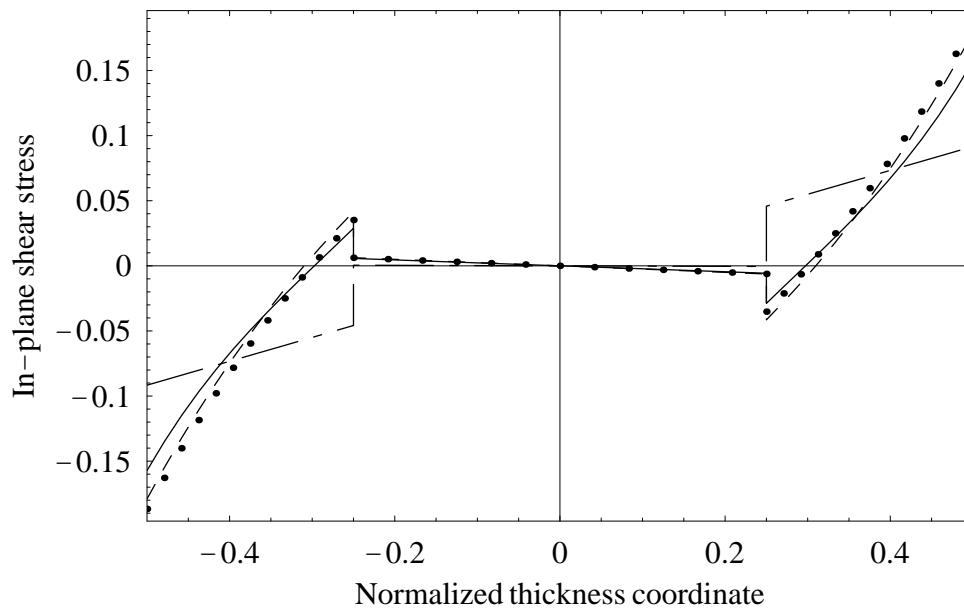


FIGURE 16:

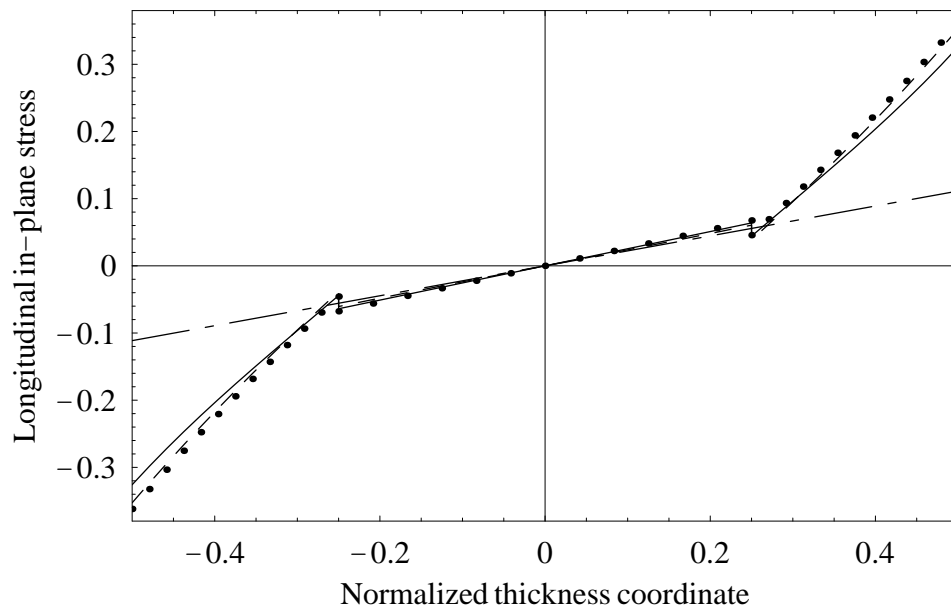


FIGURE 17:

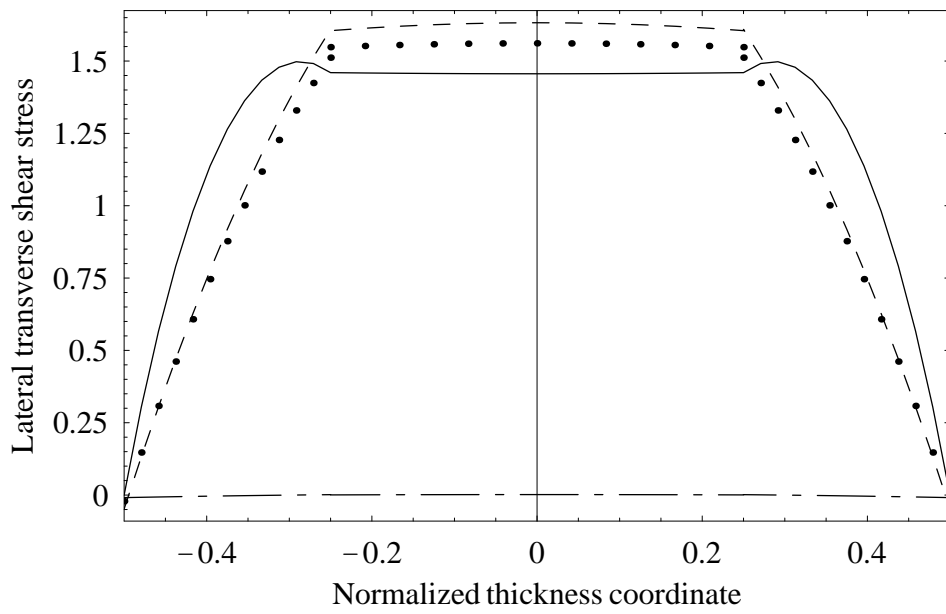


FIGURE 18:

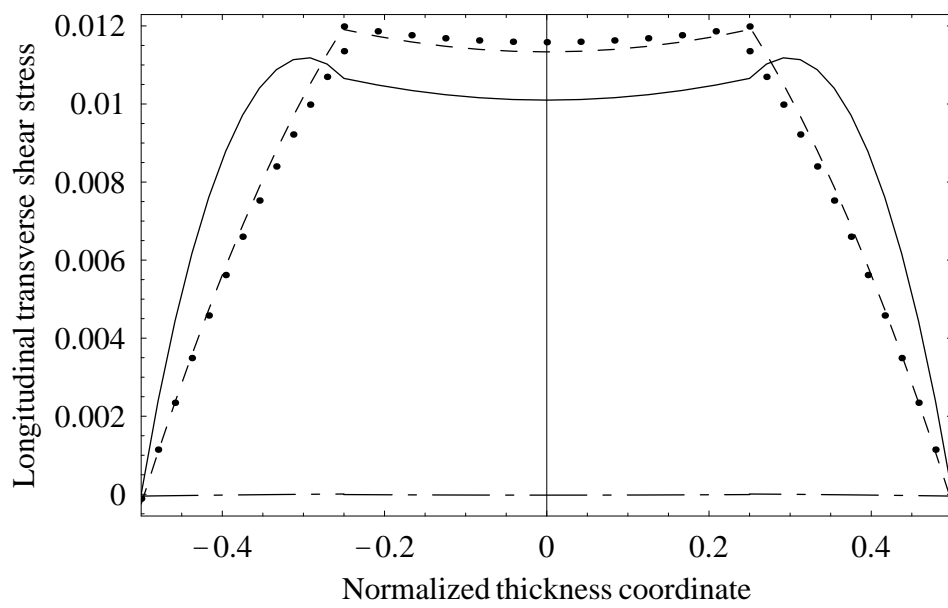


FIGURE 19:

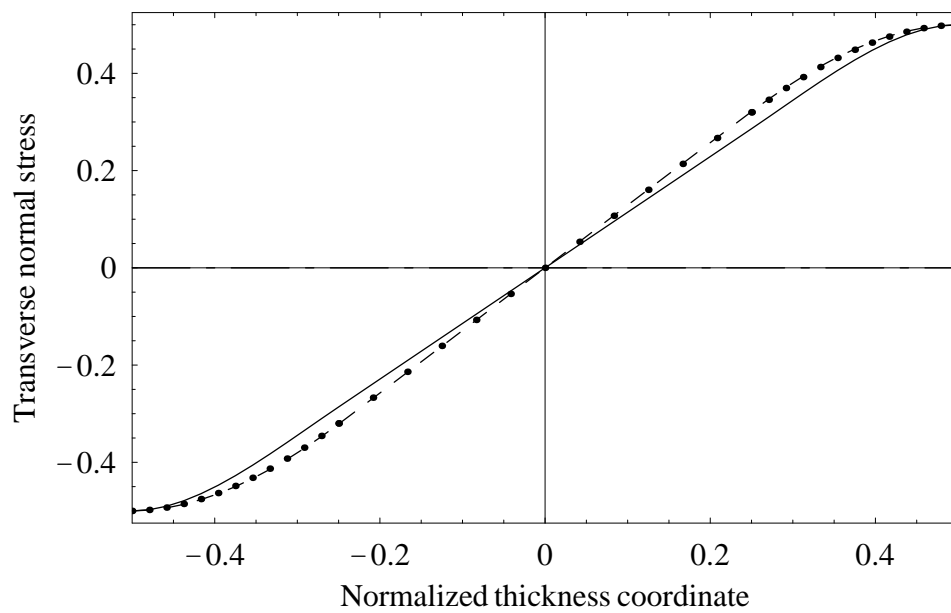


FIGURE 20:

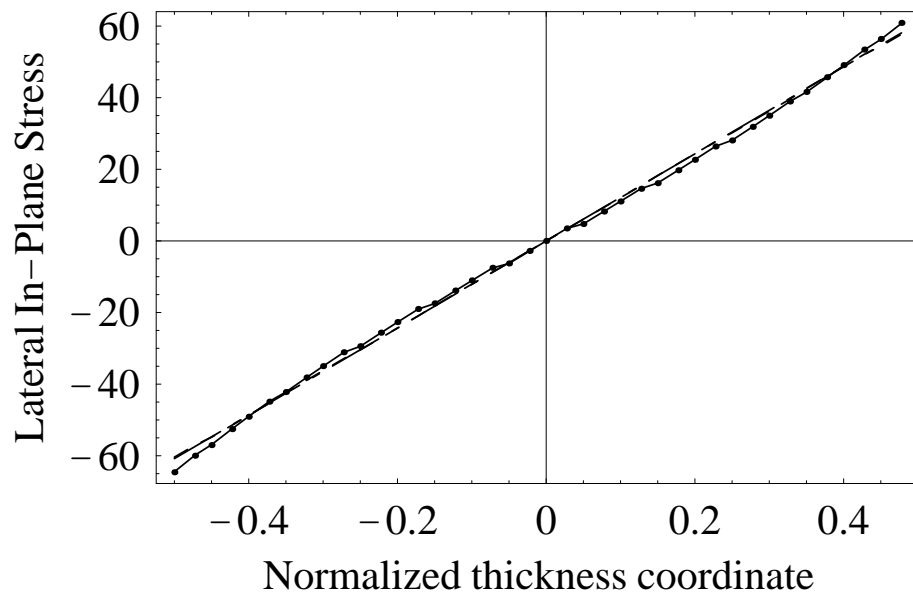


FIGURE 21:

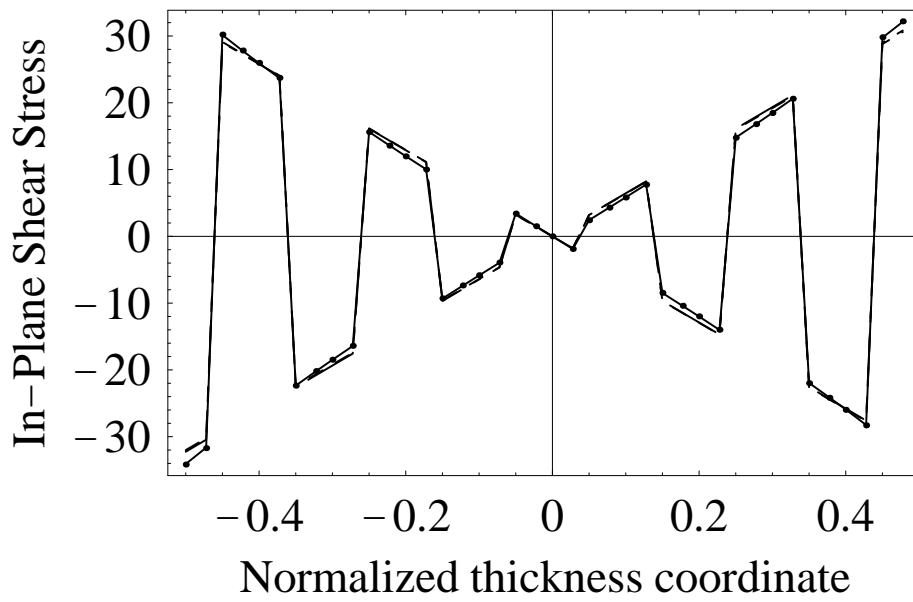


FIGURE 22:

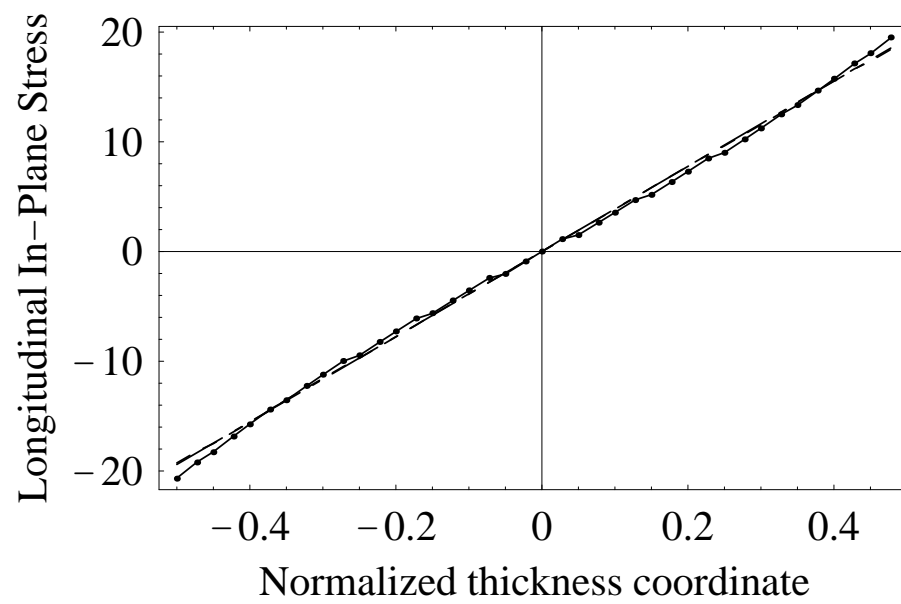


FIGURE 23:

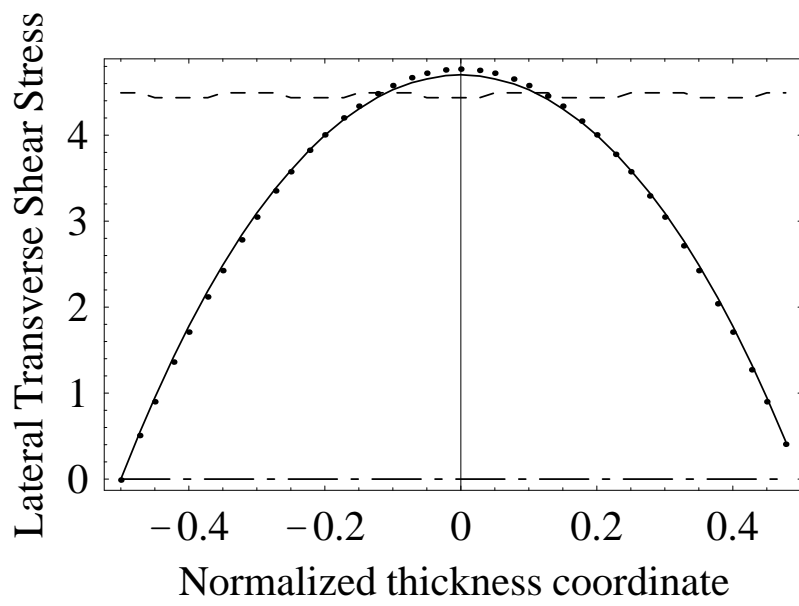


FIGURE 24:

Longitudinal Transverse Shear Stress

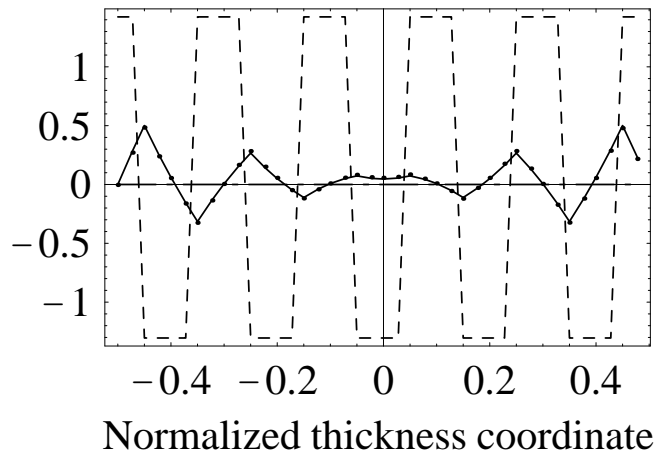


FIGURE 25:

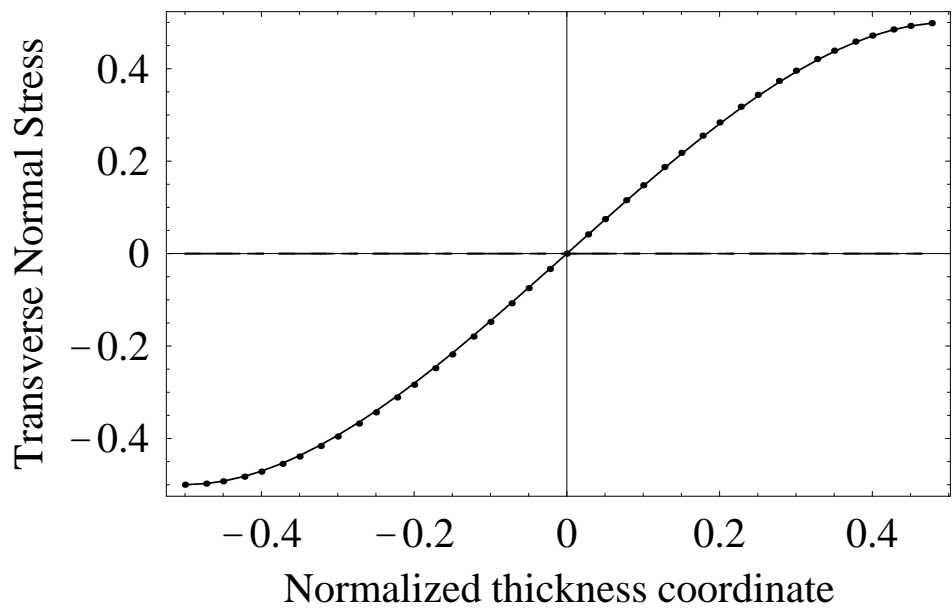


FIGURE 26:

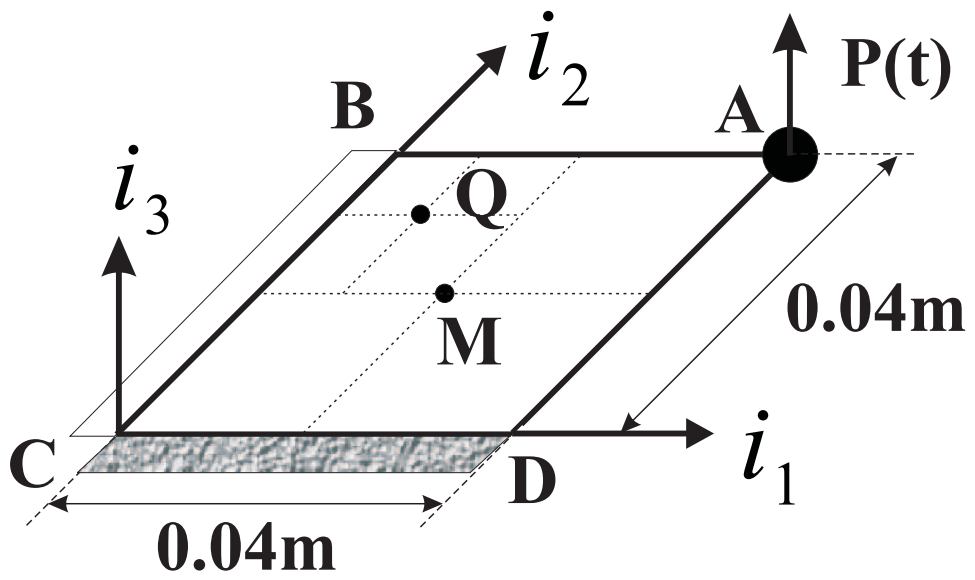


FIGURE 27:

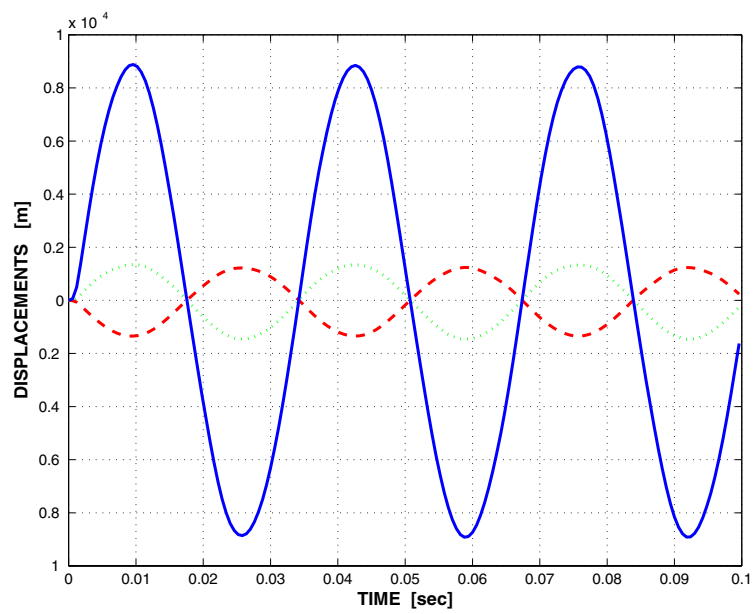


FIGURE 28:

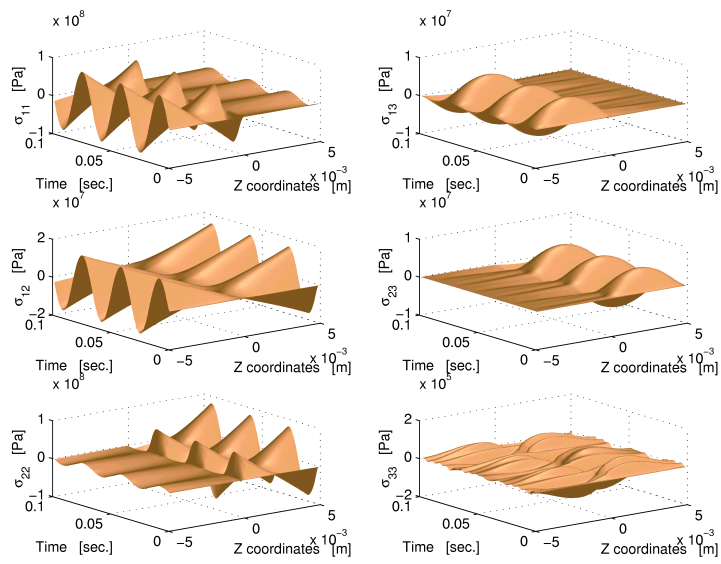


FIGURE 29:

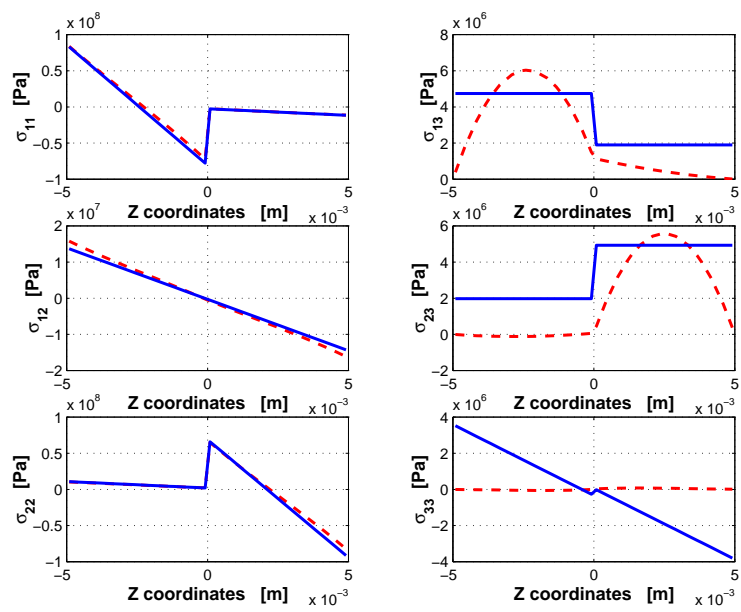


FIGURE 30:

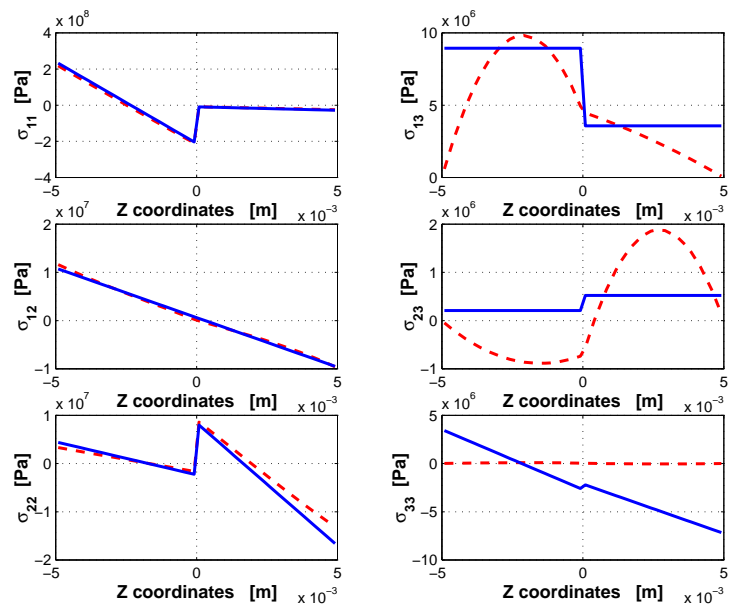


FIGURE 31: